*Current Research (2015) Newfoundland and Labrador Department of Natural Resources*
*Geological Survey, Report 15-1, pages 85-103*

# AGE AND PETROCHEMISTRY OF ROCKS FROM THE AUCOIN GOLD PROSPECT (NTS MAP AREA 13N/6), HOPEDALE BLOCK, LABRADOR: LATE ARCHEAN, ALKALI MONZODIORITE–SYENITE HOSTS PROTEROZOIC OROGENIC Au–Ag–Te MINERALIZATION

H.A.I. Sandeman and V.J. McNicoll[1]
Mineral Deposits Section
[1]Geological Survey of Canada, 601 Booth St., Ottawa, ON.

## ABSTRACT

*The Aucoin gold prospect is located 70 km west of the community of Hopedale in the southwest Archean Nain Province of Labrador (NTS 13N/6), near the southern extremity of the Torngat orogen. Mineralization consists of anastamosing, discontinuous, northeast- and northwest-trending orogenic quartz veins (typically <60 cm wide) proximal to, and within, a ≤5-m-thick, southeast-trending shear zone associated with chlorite–ankerite–epidote–talc±phengite alteration. Elevated gold correlates with silver and tellurium, reflected by argentiferous electrum and petzite ($Ag_3AuTe_2$) inclusions in sulphides and in rutile replacing ilmenite. Alteration and mineralization are hosted in four rock types. The oldest is massive to weakly foliated, medium-grained, alkali clinopyroxene–hornblende syenite that is strongly enriched in incompatible elements. The syenite is intruded by sinuous, non-chilled dykes of medium-grained, silica-undersaturated, clinopyroxene–hornblende monzodiorite that has ocean island basalt (OIB) affinity. These rocks are intruded by a ≤50-m-thick, irregular sill of medium-grained, silica-undersaturated, hornblende–porphyritic monzogabbro sharing an affinity with alkaline lamprophyres. The youngest rocks are thin (≤5 m), epidote-altered and quartz-veined, northwest-trending diabase dykes tentatively assigned to the 2235 Ma Kikkertavak (dyke) swarm.*

*U–Pb SHRIMP II zircon geochronology indicates that the syenite intruded the Mesoarchean Maggo gneiss at ≤2567 ± 4 Ma. This is contemporaneous with granulite-facies metamorphism and granitic magmatism reported in the Hopedale block, corresponding with an interval interpreted to record late Archean reworking along the Saglek–Hopedale boundary zone subsequent to amalgamation of the Nain Province. The $^{40}Ar/^{39}Ar$ step-heating analysis of phengite from altered syenite yielded a plateau age of 1873 ± 6 Ma, broadly corresponding with early events in the Torngat orogen and collision of the southeast Churchill Province core zone with the Nain Province (*ca. *1870–1850 Ma). This Paleoproterozoic interval is widely recognized as a global, 'gold fertile' metallogenetic time and highlights the potential for comparable mineralization along the Torngat orogenic front.*

## INTRODUCTION

The Aucoin prospect (UTM 602424E 6136064N: NAD27, zone 20) is located in a remote area of Labrador, ~70 km west of the community of Hopedale (NTS 13N/6; Figure 1). This part of Labrador has been mapped only at a regional scale (1:250 000 or 1:100 000: Taylor, 1977; Hill, 1982; Thomas and Morrison, 1991; Ermanovics, 1993) and modern and detailed regional geochemical and potential field data are largely lacking. The area is covered by a regional National Reconnaissance Program lake-sediment survey (one sample per 13 km$^2$: Hornbrook and Lund, 1978; Friske *et al.*, 1993) and regional, 800-m-line spacing aeromagnetic data are also available (Teskey *et al.*, 1982). Friske *et al.* (1993) noted a number of gold-in-lake sediment anomalies in the region, and publication of this report was followed by mineral claims staking by Ascot Resources Ltd. (Sandberg, 1995). Prior to these regional surveys, the only mineral exploration work comprised the Labrador-wide, reconnaissance work of Brinex and Kennco on vast mineral concessions during the 1950 to 1970s (*see* Ryan, 1984). Since then, mineral exploration in the NTS map area 13N/6 has been more vigorous, and sporadic investigations on the Aucoin prospect have continued. Work by mineral exploration companies on the prospect has generated new information about the geology of the area (Sandberg, 1995; Lehtinen and Weber, 1996; Lehtinen, 1997; Dyke and Hussey, 2003; Dyke, 2004; Hussey and Moore, 2005,

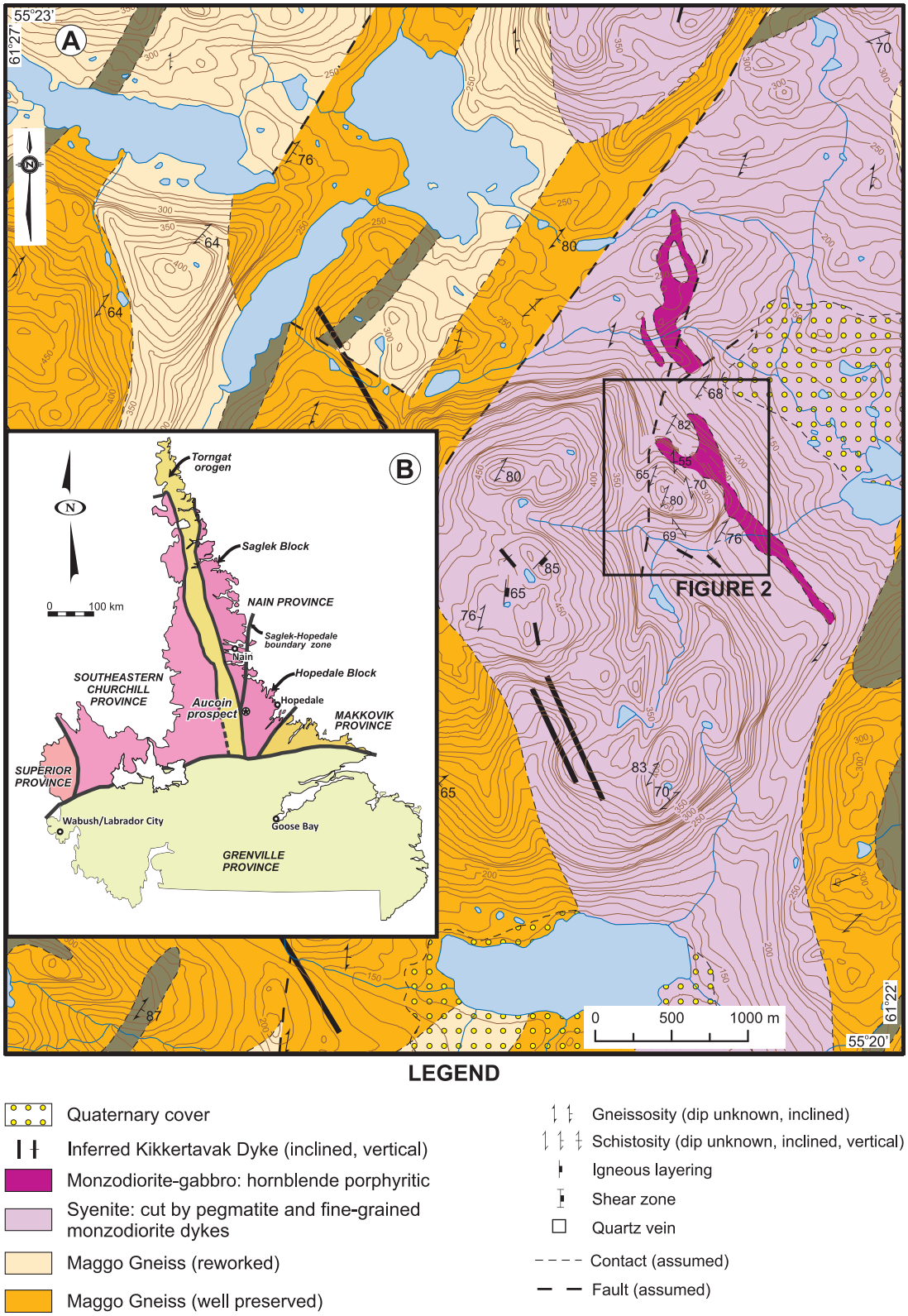


**Figure 1.** A) *Simplified, compiled geological map of the area around the Aucoin prospect. Data sources include: Hill (1982); Thomas and Morrison (1991); Ermanovics (1993); Sandberg (1995); Lehtinen and Weber (1996); Lehtinen (1997); Hussey and Moore (2005, 2006a); and* B) *Simplified lithotectonic map of Labrador showing the location of the Aucoin prospect with respect to major geological terranes and tectonic boundaries (after Wardle* et al.*, 2002).*

2006a, b). This industry-generated information, along with field, petrographic and electron microprobe imagery conducted in 2010 by the author was summarized and discussed by Sandeman and Rafuse (2011). That investigation confirmed the alkaline character of the host rocks and it was hypothesized that these rocks might form part of the Nain or Harp Lake plutonic complexes. It was tentatively suggested that gold mineralization might also be petrogenetically associated with the alkaline rocks. Altius Resources Incorporated has since conducted a reconnaissance exploration program over the prospect area, the results of which are not yet publicly available.

A preliminary U–Pb SHRIMP II age for zircon from the Aucoin syenite and a $^{40}Ar/^{39}Ar$ step-heating age date for randomly oriented phengite alteration of mineralized syenite are presented. The report also provides robust lithogeochemical data, including precious metals, for the alkaline intrusive rocks. The lithogeochemical data are available in an affiliated open file report (Sandeman, *in press*). The rocks that host the Aucoin prospect are petrochemically unusual, late Archean alkaline plutonic rocks that are, to the best of our knowledge, the first of their kind documented in Labrador. The mineralization is, however, significantly younger than the alkaline hosts and the spatial relationship is either entirely fortuitous or is a function of the relative competency of the host rocks. Further documentation of the Aucoin mineralization may help to provide alternative exploration targets for potential discovery of comparable, precious-metal mineralized systems in vastly underexplored Labrador. Examination of the regional structural controls on shear zone development and vein emplacement would be an important future avenue of research, in particular, for Paleoproterozoic, Torngat orogen-related mineralizing systems along the western margin of the Nain Province.

## REGIONAL SETTING

The Nain Province of Labrador consists of two major Archean crustal fragments, the Saglek and Hopedale blocks, which are inferred to have been juxtaposed in the late Archean, along a poorly defined, north–northeast-trending high-strain corridor termed the Saglek–Hopedale boundary zone (Figure 1: Connelly and Ryan, 1996; Wasteneys *et al.*, 1996; James *et al.*, 2002). The Aucoin prospect lies in the westernmost Hopedale block, ~10 km southeast of the Saglek–Hopedale boundary zone, but also approximately 12 km east of the north–south-oriented, tectonic boundary between the Nain craton, Torngat orogen and the southeastern Churchill Province (Figure 1, inset). The study area lies near the intersection of regional, 1:250 000 scale and 1:100 000 scale maps of Ermanovics (1993) and Thomas and Morrison (1991), respectively. The rocks around the Aucoin prospect were described as lithologically diverse, retrograde metamorphosed, relict granulite-facies granitoid rocks flanked on all sides by the heterogeneous Maggo tonalite orthogneiss (Ermanovics, 1993). The latter included a number of well preserved and reworked variants. Amphibolite units were interpreted as remnant rafts (Weekes amphibolite), inferred to represent dismembered components of the *ca.* 3000 Ma, Hunt River belt (Ermanovics, *op. cit.*; James *et al.*, 2002). Near Hopedale, these Mesoarchean rocks are crosscut by the northeast-trending, 2235 ± 2 Ma Kikkertavak dyke swarm (Ermanovics, 1993; Cadman *et al.*, 1993). In the area of the Aucoin prospect, an array of north–northwest-trending, subvertical diabase dykes were interpreted by Ermanovics (1993) as possibly representing a second, roughly orthogonal set assigned to this suite. This hypothesis, however, requires confirmation *via* U–Pb geochronology.

Twelve kilometres southwest of the Aucoin prospect, the boundary between the southeast Churchill and Nain provinces and the Torngat orogen is stitched by the anorthosite–mangerite–charnockite–granite association (AMCG) rocks of the *ca.* 1460 Ma Harp Lake intrusion (Emslie, 1980). Along the northern portion of the boundary between the Saglek and Hopedale blocks, Archean gneisses are intruded by similar rocks of the long-lived, *ca.* 1351–1292 Ma Nain Plutonic Suite (Hill, 1982; Ryan *et al.*, 1991; Thomas and Morrison, 1991) and by the *ca.* 1293–1271 Ma Flowers River intrusive complex (Hill, 1982; Brooks, 1982, 1983; Krogh, 1993; Thomas and Morrison, 1991) to the north of the Aucoin prospect. All rocks of the region, with the apparent exception of the Flowers River intrusive complex, are cut by the northeast-trending, tholeiitic Harp dykes (Hill, 1982) dated at *ca.* 1273 Ma (Cadman *et al.*, 1993).

## GEOLOGY OF THE AUCOIN PROSPECT

The hills immediately surrounding the Aucoin prospect (Figures 1 and 2) are underlain by five distinct rock types. The oldest rocks are grey, heterogeneous hornblende± clinopyroxene± biotite-bearing tonalitic Maggo orthogneiss containing centimetre- to decametre-scale screens and schlieren of fine- to medium-grained amphibolite inferred to represent dismembered Weekes amphibolite (Ermanovics, 1993; Finn, 1989; Sandeman and Rafuse, 2011). The Maggo gneiss is intruded by pink-buff coloured, generally medium-grained, massive to weakly foliated or lineated, biotite+ magnetite–ilmenite+clinopyroxene+hornblende syenite (Plate 1A). The syenite contains relatively common, irregular lenses or magmatic enclaves of fine- to medium-grained monzodiorite, and locally varies on the outcrop-scale to quartz syenite or patches and veins of syenogranite pegmatite (*see* Hussey and Moore, 2005). The syenite contains

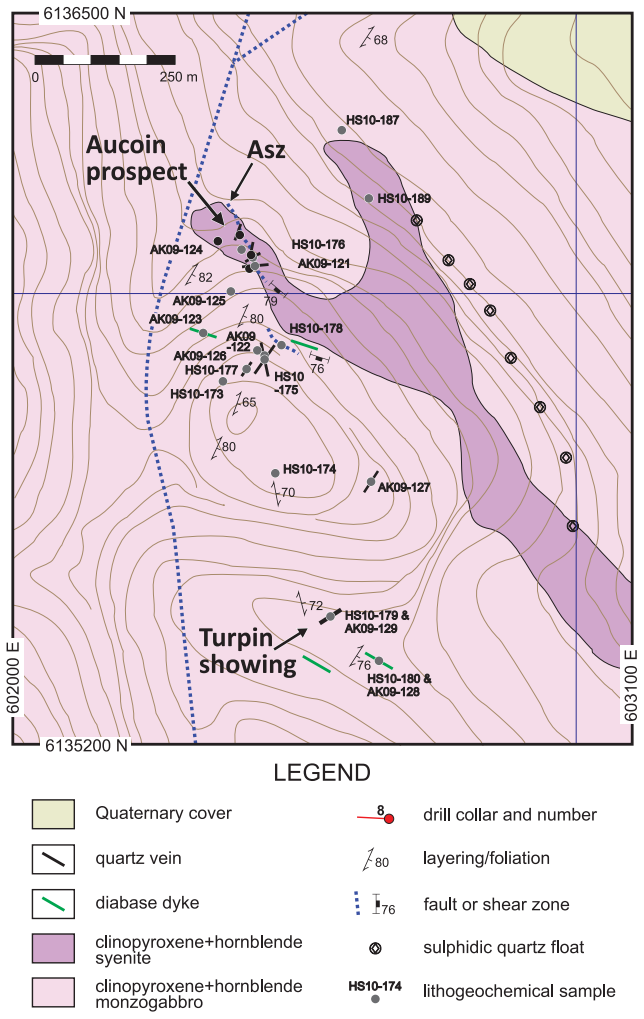


**Figure 2.** *Detailed geology of the Aucoin prospect showing the locations of industry drill collars and lithogeochemical samples from this investigation.*

abundant, large anhedral grains of perthite and very minor quartz. Accessory phases include: common anhedral grains of ilmenite and magnetite, locally mantled by anhedral secondary titanite and uncommon, subhedral blocky apatite and zircon.

Syenite is commonly crosscut by generally thin (<2 m) sinuous, anastamosing dykes of fine-grained biotite+magnetite–ilmenite+hornblende+clinopyroxene monzodiorite. These lack chill margins, but have relatively abrupt, locally scalloped and/or gradational contacts with the host syenite. The monzodiorite comprises: ~45% feldspar consisting of abundant untwinned or simply twinned orthoclase with less common lamellar twinned plagioclase; ~20% elongate, euhedral, dark-green to pale-green pleochroic Ferroan hornblende; ~20% prismatic, pale-green to yellow titaniferous clinopyroxene; ~10% anhedral grains of integrown magnetite-ilmenite and; ≤5% small anhedral biotite (Plate 1B). Short stubby apatite grains are the only noted accessory mineral.

Immediately north and east of the Aucoin prospect is an irregular, ≤50-m-thick, southeast-trending sill or sheet of green-black, medium- to coarse-grained, hornblende–porphyritic magnetite–ilmenite+clinopyroxene monzogabbro (Plate 1C). This rock type contains euhedral, poikilitic (≤6 mm) phenocrysts of brown-green Ferroan hornblende (Barkevikite?) having green mantles, euhedral, pink to pale-orange titaniferous clinopyroxene (≤2 mm) and, abundant, subhedral magnetite and ilmenite and intergrown ilmenite–magnetite (≤2 mm). These are all surrounded by a matrix consisting of oikocrystic, lamellar-twinned plagioclase, with less common potassium feldspar and rare anhedral pyrite and chalcopyrite. Abundant euhedral apatite and rare zircon are the only other notable accessory phases. Outcrop exposures and drillcore suggest that the monzogabbro sill trends southeast, dips moderately southwest and passes relatively abruptly upward into syenite.

All of these rocks are crosscut by two sets of green-black, subvertical mafic dykes that have prominent chill margins. The most common variety of dyke trends north–northwest (*ca.* 150-120°/90°) and comprises weakly plagioclase–porphyritic, ilmenite–magnetite+actinolite (clinopyroxene)-bearing diabase (Plate 1D). These were tentatively interpreted as a second, orthogonal set of dykes correlated with the Kikkertavak (dyke) swarm (Ermanovics, 1993). A single, southwest-trending (230°/80°NW) green dyke (≤25 cm wide) was noted by Hussey and Moore (2005), but not during this investigation. Whether the southwest-trending dyke is contemporaneous with the northwest-trending set is unknown, but its orientation resembles that of the younger Harp dykes.

The undulated upper contact zone between the syenite and the monzogabbro sill comprises a sheared, quartz-veined and phengite+chlorite+ankerite±epidote±talc-altered zone that hosts much of the gold mineralization and is termed the Aucoin shear zone (ASZ). In contrast to the coarse-grained igneous rocks and diabase dykes, the ASZ is moderate to strongly schistose. The orientation of the ASZ, as determined from drillhole intersections (Sandberg, 1995) is ~158/44°SW, however, a similar, strongly schistose zone with abundant sigmoidal quartz veinlets was noted at surface (location HS10-178: Figure 2) and trends ~288/76°NE. Quartz veins, proximal to the shear zones, exhibit two distinct orientations. Deformed, thin (≤20 cm), discontinuous, ribboned and sigmoidal, white quartz veins generally parallel the northwest-trending fabric in the shear zones (*see* Figure 6A; Sandeman and Rafuse, 2011). In contrast, wider (typically ≤60 cm) white and massive, north-northeast-trending quartz veins occur in syenite and monzodiorite in

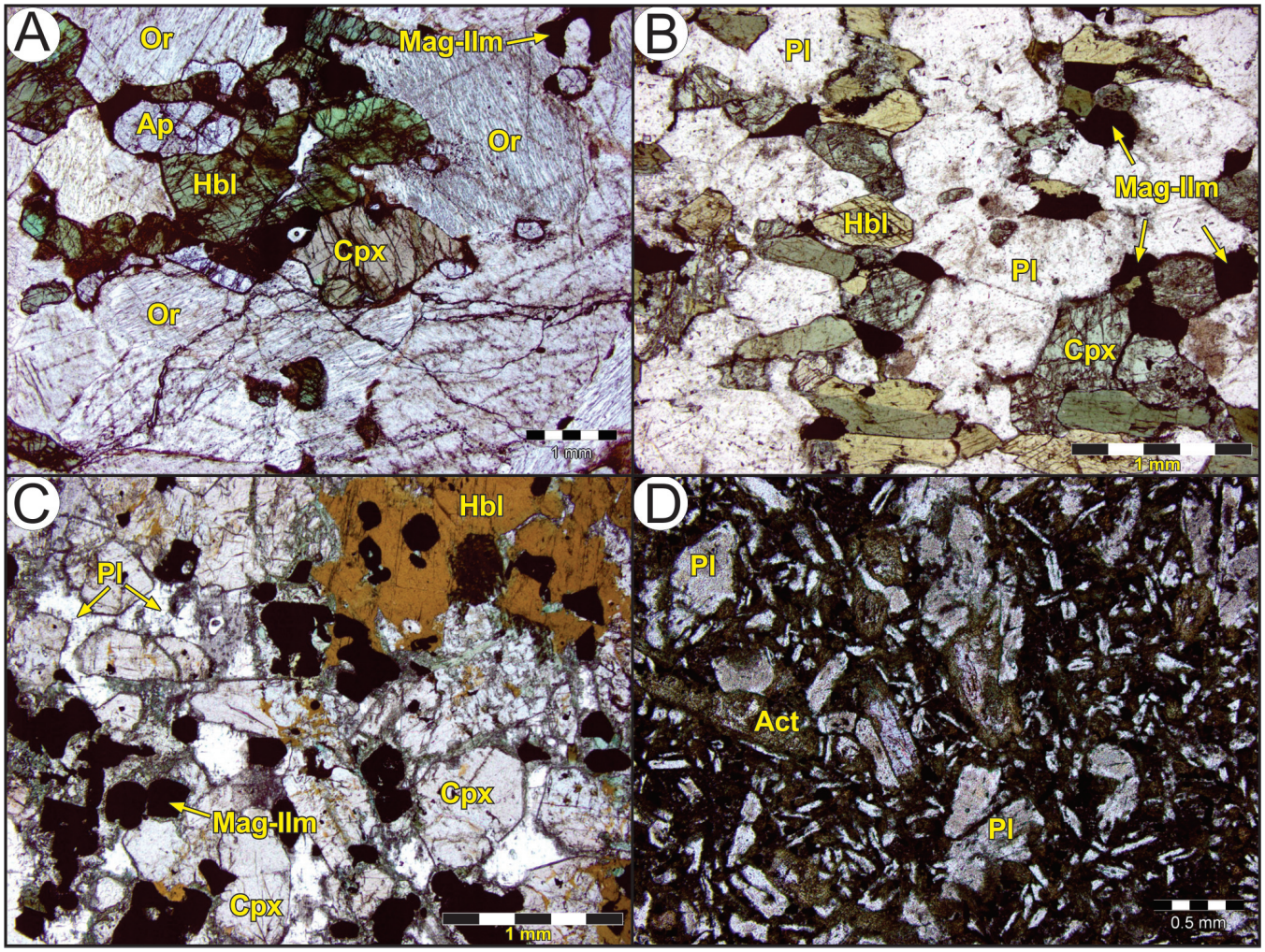


**Plate 1.** *Photomicrographs of representative fresh rock-types that host the Aucoin prospect. A) Weakly foliated, medium-grained clinopyroxene–hornblende syenite (HS10-180A); B) Medium-grained hornblende–clinopyroxene monzodiorite dyke cuts syenite (HS10-180B); C) Medium-grained hornblende porphyritic monzogabbro intersected in drillhole AR96-04 (AR96-04_25.3 m); and D) Fine-grained, green, diabase dyke with chill margins (HS10-180C). Mineral abbreviations after Kretz (1983).*

the hanging wall of the shear zones (southwest). The veins and their adjacent altered wallrock locally contain up to 10-15% disseminated euhedral pyrite along with minor chalcopyrite and rare galena. Visible gold has been reported from the sulphidic margins of some of these veins (Sandberg, 1995; Dyke, 2004) and grab samples have yielded up to 477 g/t Au and >100 g/t Ag (Hussey and Moore, 2005).

## U–Pb GEOCHRONOLOGY

### ANALYTICAL METHODS

Sensitive High Resolution Ion MicroProbe (SHRIMP II) analyses were conducted at the Geological Survey of Canada using analytical and data reduction procedures described by Stern (1997) and Stern and Amelin (2003). Zircons from the Aucoin syenite sample (GSC lab number z10413) and fragments of the GSC laboratory zircon standard (z6266 zircon, with $^{206}Pb/^{238}U$ age = 559 Ma ) were cast in an epoxy grain mount (GSC mount IP587), polished with diamond compound to reveal the grain centres, and photographed in transmitted light. The mount was evaporatively coated with 10 nm of high purity Au, and the internal features of the zircons were characterized with backscattered electrons (BSE) and cathodoluminescence (CL) utilizing a scanning electron microscope (SEM). Analyses were conducted using a primary beam projected onto the zircons with an elliptical spot size of 13 x 16 µm (K100). The count rates of ten isotopes of $Zr^+$, $U^+$, $Th^+$, and $Pb^+$ in zircon were sequentially measured with a single electron multiplier. Off-line data processing was accomplished using customized in-house software. The SHRIMP II analytical data are present-

ed in Table 1. Common-Pb-corrected ratios and ages are reported with 1σ analytical errors, which incorporate an external uncertainty of 1.0% in calibrating the standard zircon (*see* Stern and Amelin, 2003). Analyses of a secondary zircon standard (Temora 2) were interspersed between the sample analyses to verify the accuracy of the U–Pb calibration. Using the calibration defined by the z6266 standard, the weighted mean $^{206}Pb/^{238}U$ age of the analyses of Temora 2 zircon on the grain mount was determined to be 415.2 ± 3.4 Ma. The accepted $^{206}Pb/^{238}U$ age of Temora 2 is 416.5 ± 0.22 Ma, based on 21 isotope dilution fractions (Black *et al.*, 2005). Isoplot v. 3.00 (Ludwig, 2003) was used to generate the concordia and cumulative probability plots (Figure 3). The error ellipses on the concordia diagram are displayed at 2σ.

**RESULTS FOR SAMPLE AR96-01-65M (Z10413)**

A sample of clinopyroxene–hornblende syenite (AR96-01-65m (z10413): UTM NAD 27 zone 20 602400E - 6136000N) was collected for U–Pb geochronology and lithogeochemistry from diamond-drill core, 30 m down-hole from the contact between carbonate-altered hornblende–porphyritic monzogabbro and medium-grained hornblende–clinopyroxene syenite. This fresh syenite is petrographically and geochemically similar to the mineralized syenite.

Abundant zircon grains of variable morphology were retrieved from the sample including euhedral prismatic and stubby prismatic grains, equant multifaceted crystals, as well as subrounded grains. The BSE–SEM images reveal faint growth zoning in many of the zircon grains (Figure 3A). The U–Pb SHRIMP II analyses yield a wide range of Archean data (2.74–2.54 Ga: n=49, Table 1, Figure 3). A weighted average of the $^{207}Pb/^{206}Pb$ ages of the youngest cluster of concordant, overlapping data is calculated to be 2567 ± 4 (MSWD = 1.1, probability of fit = 0.38, n=11). It is possible that this represents the age of the syenite, however, as there is a large range in the determined ages, it is possible that all of the zircons analyzed are inherited in origin. The resultant age of 2567 ± 4 Ma is, therefore, interpreted to represent a maximum age for the Aucoin syenite.

**$^{40}Ar/^{39}Ar$ THERMOCHRONOLOGY**

The $^{40}Ar/^{39}Ar$ age was obtained at Queen's University $^{40}Ar/^{39}Ar$ Thermochronology Laboratory. Mineral separates and flux-monitors (standards) are wrapped in Al-foil, stacked sequentially into an 8.5-cm-long and 2.0-cm-diameter Al irradiation capsule, and then irradiated with fast neutrons in position 8D of the McMaster Nuclear Reactor (Hamilton, Ontario) for a duration of 72 h (at 3 MWH). Packets of flux monitors are located at ~0.5 cm intervals along the irradiation container and the J-value for an individual sample is determined by least-squares, second-order polynomial interpolation using replicate analyses of splits for each monitor position in the capsule.

The samples are loaded into flat-bottomed pits in a copper sample-holder and placed beneath the ZnS view-port of a small, bakeable, stainless-steel chamber connected to an ultra-high vacuum purification system. Following bake out at 100°C, a 30 watt New Wave Research MIR 10-30 $CO_2$ laser with a faceted lens is used to heat samples for ~3 minutes at increasing percent power settings (2 to 45%; beam diameter 3 mm). After purification using hot and cold SAES C50 getters (for ~5 minutes), the evolved gas is admitted to an MAP 216 mass spectrometer, with a Bäur Signer source and an analog electron multiplier (set to a gain of 100 over the Faraday detector).

Measured argon-isotope peak heights are extrapolated to zero-time and corrected for discrimination using a $^{40}Ar/^{36}Ar$ atmospheric ratio of 295.5 and measured ratios of atmospheric argon. Blanks, measured routinely, are subtracted from the subsequent sample gas-fractions. The extraction blanks are typically $<10 \times 10^{-13}$, $<0.5 \times 10^{-13}$, $<0.5 \times 10^{-13}$, and $<0.5 \times 10^{-13}$ $cm^{-3}$ STP for masses 40, 39, 37, and 36, respectively. The $^{39}Ar$ and $^{37}Ar$ are corrected for radioactive decay during and after irradiation. Corrections are made for neutron-induced $^{40}Ar$ from potassium, $^{39}Ar$ and $^{36}Ar$ from calcium, and $^{36}Ar$ from chlorine (Roddick, 1983; Onstott *et al.*, 1991). Dates and errors are calculated using the procedure of Dalrymple *et al.* (1981) and the constants of Steiger and Jäger (1977). Plateau and inverse isotope correlation dates are calculated using ISOPLOT v. 3.60 (Ludwig, 2008). A plateau is herein defined as 3 or more contiguous steps containing >50% of the $^{39}Ar$ released, with a probability of fit >0.01 and MSWD <2.

Errors shown in Table 2 and in Figure 4B represent the analytical precision at 2σ, assuming that the errors in the ages of the flux monitors are zero. This is suitable for comparing within-spectrum variation and determining which steps form a plateau (*e.g.*, McDougall and Harrison, 1988, page 89). The dates and J-values are referenced to GA1550 biotite (98.5 Ma; Spell and McDougall, 2003) and Hb3Gr hornblende (PP-20; 1073.6 Ma; Jourdan *et al.*, 2006). The gas steps 4 to 21 were used in the calculation of the plateau age and are marked by bold type in Table 2 and by shaded boxes in Figure 4B.

The $^{40}Ar/^{39}Ar$ laser step-heating age was determined for a white mica grain separate (175-250 μm) extracted from sample HS10-177B, a medium-grained, altered syenite that occurs in the structural hanging wall of the Aucoin prospect (Figure 2). This sample, which yielded 102 ppb Au, is dom-

**Table 1.** SHRIMP II U/Pb zircon results

AR96-01-65m (GSC lab# z10413; UTM NAD27, Zone 20, 602400E - 6136000N); GSC mount# IP587

| Spot name | U (ppm) | Th (ppm) | Th/U | $^{206}Pb^*$ (ppm) | $^{204}Pb/^{206}Pb$ | $\pm^{204}Pb/^{206}Pb$ | f(206)$^{204}$ | $^{208*}Pb/^{206*}Pb$ | $\pm^{208*}Pb/^{206*}Pb$ | $^{207*}Pb/^{235}U$ | $\pm^{207*}Pb/^{235}U$ | $^{206*}Pb/^{238}U$ | $\pm^{206*}Pb/^{238}U$ | Corr Coeff | $^{207*}Pb/^{206*}Pb$ | $\pm^{207*}Pb/^{206*}Pb$ | Apparent Ages (Ma) $^{206}Pb/^{238}U$ | $\pm^{206}Pb/^{238}U$ | $^{207}Pb/^{206}Pb$ | $\pm^{207}Pb/^{206}Pb$ | Disc. (%) |
|---|---|---|---|---|---|---|---|---|---|---|---|---|---|---|---|---|---|---|---|---|---|
| 10413-14.1 | 315 | 75 | 0.24 | 144 | 1.35E-5 | 4.04E-6 | 0.0002 | 0.0673 | 0.0019 | 13.908 | 0.152 | 0.5331 | 0.0056 | 0.9585 | 0.1892 | 0.0006 | 2755 | 23.5 | 2735 | 5.1 | -0.9 |
| 10413-51.1 | 244 | 99 | 0.40 | 113 | 2.81E-5 | 3.35E-5 | 0.0005 | 0.1204 | 0.0027 | 13.959 | 0.171 | 0.5397 | 0.0063 | 0.9443 | 0.1876 | 0.0008 | 2782 | 26.2 | 2721 | 6.7 | -2.8 |
| 10413-49.1 | 284 | 143 | 0.50 | 117 | 2.22E-5 | 4.83E-6 | 0.0004 | 0.1459 | 0.0030 | 11.285 | 0.127 | 0.4802 | 0.0051 | 0.9491 | 0.1704 | 0.0006 | 2528 | 22.4 | 2562 | 5.9 | 1.6 |
| 10413-52.1 | 270 | 94 | 0.35 | 114 | 1.77E-5 | 5.43E-6 | 0.0003 | 0.1014 | 0.0024 | 11.889 | 0.132 | 0.4931 | 0.0052 | 0.9444 | 0.1749 | 0.0006 | 2584 | 22.4 | 2605 | 6.1 | 1.0 |
| 10413-53.1 | 329 | 122 | 0.37 | 146 | --- | --- | 0.0000 | 0.1121 | 0.0023 | 13.189 | 0.144 | 0.5146 | 0.0054 | 0.9555 | 0.1859 | 0.0006 | 2676 | 22.9 | 2706 | 5.3 | 1.3 |
| 10413-54.1 | 170 | 141 | 0.83 | 77 | -1.73E-5 | -1.32E-5 | -0.0003 | 0.2506 | 0.0047 | 13.480 | 0.157 | 0.5258 | 0.0057 | 0.9251 | 0.1859 | 0.0008 | 2724 | 24.0 | 2707 | 7.3 | -0.8 |
| 10413-56.1 | 280 | 187 | 0.67 | 119 | 1.47E-5 | 4.29E-6 | 0.0003 | 0.1970 | 0.0034 | 11.871 | 0.133 | 0.4947 | 0.0053 | 0.9459 | 0.1740 | 0.0006 | 2591 | 22.7 | 2597 | 6.1 | 0.3 |
| 10413-55.1 | 389 | 112 | 0.29 | 173 | 8.58E-6 | 2.65E-6 | 0.0001 | 0.0858 | 0.0019 | 13.234 | 0.143 | 0.5173 | 0.0054 | 0.9601 | 0.1855 | 0.0006 | 2688 | 22.8 | 2703 | 5.0 | 0.7 |
| 10413-58.1 | 411 | 199 | 0.49 | 182 | 8.29E-6 | 3.20E-6 | 0.0001 | 0.1369 | 0.0023 | 13.310 | 0.144 | 0.5162 | 0.0054 | 0.9650 | 0.1870 | 0.0005 | 2683 | 22.9 | 2716 | 4.7 | 1.5 |
| 10413-57.1 | 166 | 100 | 0.60 | 69 | 2.74E-5 | 8.97E-6 | 0.0005 | 0.1706 | 0.0041 | 11.333 | 0.147 | 0.4851 | 0.0059 | 0.9274 | 0.1694 | 0.0008 | 2549 | 25.4 | 2552 | 8.2 | 0.1 |
| 10413-1.1 | 243 | 142 | 0.59 | 101 | 2.71E-5 | 2.35E-5 | 0.0005 | 0.1821 | 0.0051 | 11.511 | 0.140 | 0.4846 | 0.0052 | 0.8726 | 0.1723 | 0.0010 | 2547 | 22.4 | 2580 | 10.0 | 1.5 |
| 10413-2.1 | 222 | 208 | 0.94 | 97 | 6.19E-5 | 1.89E-5 | 0.0011 | 0.2792 | 0.0047 | 13.070 | 0.150 | 0.5107 | 0.0054 | 0.9280 | 0.1856 | 0.0008 | 2660 | 23.2 | 2704 | 7.1 | 2.0 |
| 10413-4.1 | 277 | 137 | 0.49 | 123 | 1.47E-5 | 4.09E-6 | 0.0003 | 0.1387 | 0.0029 | 12.828 | 0.179 | 0.5183 | 0.0070 | 0.9643 | 0.1795 | 0.0007 | 2692 | 29.6 | 2648 | 6.1 | -2.0 |
| 10413-5.1 | 359 | 518 | 1.44 | 157 | --- | --- | 0.0000 | 0.4369 | 0.0057 | 13.173 | 0.178 | 0.5097 | 0.0066 | 0.9563 | 0.1875 | 0.0007 | 2655 | 28.2 | 2720 | 6.5 | 2.9 |
| 10413-7.1 | 263 | 289 | 1.10 | 121 | 1.71E-5 | 6.20E-6 | 0.0003 | 0.3168 | 0.0057 | 13.718 | 0.156 | 0.5354 | 0.0057 | 0.9418 | 0.1858 | 0.0007 | 2764 | 24.1 | 2706 | 6.3 | -2.7 |
| 10413-6.1 | 201 | 104 | 0.52 | 81 | --- | --- | 0.0000 | 0.1515 | 0.0036 | 11.160 | 0.129 | 0.4678 | 0.0050 | 0.9240 | 0.1730 | 0.0008 | 2474 | 21.9 | 2587 | 7.4 | 5.3 |
| 10413-9.1 | 293 | 156 | 0.53 | 130 | 1.06E-5 | 7.34E-6 | 0.0002 | 0.1607 | 0.0030 | 13.174 | 0.158 | 0.5140 | 0.0059 | 0.9572 | 0.1859 | 0.0006 | 2674 | 25.2 | 2706 | 5.7 | 1.5 |
| 10413-10.1 | 232 | 117 | 0.50 | 96 | 1.80E-5 | 6.55E-6 | 0.0003 | 0.1500 | 0.0033 | 11.272 | 0.128 | 0.4817 | 0.0051 | 0.9332 | 0.1697 | 0.0007 | 2535 | 22.2 | 2555 | 6.8 | 1.0 |
| 10413-12.1 | 238 | 148 | 0.62 | 103 | 2.08E-5 | 2.74E-5 | 0.0004 | 0.1761 | 0.0035 | 12.884 | 0.162 | 0.5039 | 0.0060 | 0.9410 | 0.1854 | 0.0008 | 2631 | 25.6 | 2702 | 7.0 | 3.2 |
| 10413-11.1 | 279 | 156 | 0.56 | 119 | 6.31E-6 | 3.44E-6 | 0.0001 | 0.1651 | 0.0031 | 11.715 | 0.144 | 0.4956 | 0.0058 | 0.9546 | 0.1714 | 0.0006 | 2595 | 25.1 | 2572 | 6.1 | -1.1 |
| 10413-13.1 | 197 | 99 | 0.50 | 84 | 3.39E-5 | 4.79E-5 | 0.0006 | 0.1520 | 0.0035 | 11.818 | 0.143 | 0.4973 | 0.0053 | 0.8872 | 0.1724 | 0.0010 | 2602 | 23.0 | 2581 | 9.3 | -1.0 |
| 10413-38.1 | 357 | 200 | 0.56 | 162 | 1.21E-5 | 3.10E-6 | 0.0002 | 0.1642 | 0.0026 | 13.593 | 0.147 | 0.5269 | 0.0055 | 0.9600 | 0.1871 | 0.0006 | 2728 | 23.1 | 2717 | 5.0 | -0.5 |
| 10413-37.1 | 219 | 103 | 0.47 | 90 | -1.45E-5 | -1.38E-5 | -0.0003 | 0.1462 | 0.0034 | 11.297 | 0.143 | 0.4794 | 0.0057 | 0.9406 | 0.1709 | 0.0007 | 2525 | 24.9 | 2567 | 7.2 | 2.0 |
| 10413-41.1 | 143 | 75 | 0.52 | 61 | -2.18E-5 | -1.45E-5 | -0.0004 | 0.1568 | 0.0043 | 11.748 | 0.143 | 0.4931 | 0.0054 | 0.9016 | 0.1728 | 0.0009 | 2584 | 23.3 | 2585 | 8.8 | 0.0 |
| 10413-39.1 | 310 | 176 | 0.57 | 135 | --- | --- | 0.0000 | 0.1703 | 0.0038 | 12.776 | 0.284 | 0.5077 | 0.0095 | 0.8395 | 0.1825 | 0.0022 | 2647 | 40.5 | 2676 | 20.0 | 1.3 |
| 10413-43.1 | 184 | 99 | 0.54 | 78 | --- | --- | 0.0000 | 0.1615 | 0.0039 | 11.714 | 0.137 | 0.4951 | 0.0053 | 0.9190 | 0.1716 | 0.0008 | 2593 | 23.0 | 2573 | 7.7 | -0.9 |
| 10413-45.1 | 141 | 70 | 0.50 | 60 | 3.08E-5 | 9.14E-6 | 0.0005 | 0.1371 | 0.0039 | 12.567 | 0.157 | 0.4991 | 0.0057 | 0.9173 | 0.1826 | 0.0009 | 2610 | 24.6 | 2677 | 8.2 | 3.0 |
| 10413-46.1 | 190 | 112 | 0.59 | 80 | 3.13E-5 | 5.90E-5 | 0.0005 | 0.1649 | 0.0047 | 11.566 | 0.146 | 0.4912 | 0.0054 | 0.8699 | 0.1708 | 0.0011 | 2576 | 23.3 | 2565 | 10.4 | 0.5 |
| 10413-47.1 | 251 | 150 | 0.60 | 115 | --- | --- | 0.0000 | 0.1682 | 0.0033 | 13.586 | 0.157 | 0.5326 | 0.0056 | 0.9162 | 0.1850 | 0.0009 | 2752 | 23.7 | 2698 | 7.6 | -2.5 |
| 10413-48.1 | 270 | 141 | 0.52 | 110 | 6.22E-5 | 1.76E-5 | 0.0011 | 0.1479 | 0.0030 | 11.220 | 0.158 | 0.4756 | 0.0064 | 0.9577 | 0.1711 | 0.0007 | 2508 | 28.0 | 2568 | 6.8 | 2.8 |
| 10413-16.1 | 482 | 278 | 0.58 | 199 | 2.70E-5 | 9.10E-6 | 0.0005 | 0.1678 | 0.0024 | 11.201 | 0.120 | 0.4797 | 0.0049 | 0.9619 | 0.1693 | 0.0005 | 2526 | 21.5 | 2551 | 4.9 | 1.2 |
| 10413-17.1 | 235 | 136 | 0.58 | 107 | -2.22E-5 | -1.79E-07 | -0.0004 | 0.1618 | 0.0034 | 13.161 | 0.153 | 0.5318 | 0.0058 | 0.9407 | 0.1795 | 0.0007 | 2749 | 24.4 | 2648 | 6.5 | -4.7 |
| 10413-18.1 | 355 | 220 | 0.62 | 150 | 1.65E-5 | 8.49E-6 | 0.0003 | 0.1836 | 0.0028 | 11.617 | 0.126 | 0.4914 | 0.0051 | 0.9544 | 0.1715 | 0.0006 | 2577 | 22.0 | 2572 | 5.4 | 0.2 |
| 10413-20.1 | 200 | 87 | 0.43 | 90 | 1.70E-5 | 6.10E-6 | 0.0003 | 0.1288 | 0.0030 | 13.497 | 0.157 | 0.5254 | 0.0058 | 0.9411 | 0.1863 | 0.0007 | 2722 | 24.3 | 2710 | 6.5 | -0.6 |
| 10413-19.1 | 246 | 157 | 0.64 | 105 | 1.15E-5 | 4.01E-6 | 0.0002 | 0.1855 | 0.0034 | 11.705 | 0.137 | 0.4948 | 0.0055 | 0.9454 | 0.1716 | 0.0007 | 2591 | 23.7 | 2573 | 6.4 | -0.9 |
| 10413-21.1 | 430 | 210 | 0.49 | 196 | 1.02E-5 | 3.01E-6 | 0.0002 | 0.1397 | 0.0022 | 13.593 | 0.145 | 0.5296 | 0.0055 | 0.9670 | 0.1862 | 0.0005 | 2740 | 23.0 | 2709 | 4.5 | -1.4 |
| 10413-22.1 | 332 | 47 | 0.14 | 148 | 1.19E-5 | 3.95E-6 | 0.0002 | 0.0404 | 0.0013 | 12.999 | 0.163 | 0.5178 | 0.0062 | 0.9508 | 0.1821 | 0.0007 | 2690 | 26.3 | 2672 | 6.4 | -0.8 |
| 10413-23.1 | 175 | 141 | 0.81 | 75 | 2.52E-5 | 8.27E-6 | 0.0004 | 0.2366 | 0.0046 | 12.917 | 0.153 | 0.4976 | 0.0055 | 0.9287 | 0.1883 | 0.0008 | 2603 | 23.5 | 2727 | 7.2 | 5.5 |
| 10413-24.1 | 145 | 112 | 0.78 | 60 | 3.47E-5 | 1.02E-5 | 0.0006 | 0.2279 | 0.0054 | 12.647 | 0.190 | 0.4846 | 0.0053 | 0.7299 | 0.1893 | 0.0019 | 2547 | 23.1 | 2736 | 16.9 | 8.3 |
| 10413-27.1 | 174 | 81 | 0.47 | 73 | 4.78E-5 | 4.95E-5 | 0.0008 | 0.1375 | 0.0034 | 11.603 | 0.141 | 0.4902 | 0.0053 | 0.8821 | 0.1717 | 0.0010 | 2571 | 22.8 | 2574 | 9.6 | 0.1 |
| 10413-31.1 | 267 | 41 | 0.15 | 112 | 1.36E-5 | 5.05E-6 | 0.0002 | 0.0417 | 0.0015 | 11.736 | 0.136 | 0.4893 | 0.0054 | 0.9499 | 0.1739 | 0.0006 | 2568 | 23.4 | 2596 | 6.1 | 1.3 |
| 10413-29.1 | 82 | 69 | 0.84 | 37 | --- | --- | 0.0000 | 0.2582 | 0.0069 | 13.760 | 0.200 | 0.5295 | 0.0069 | 0.9041 | 0.1885 | 0.0012 | 2740 | 29.3 | 2729 | 10.2 | 0.5 |
| 10413-30.1 | 246 | 125 | 0.51 | 113 | 6.78E-6 | 3.70E-6 | 0.0001 | 0.1461 | 0.0030 | 13.975 | 0.181 | 0.5343 | 0.0062 | 0.9014 | 0.1897 | 0.0011 | 2760 | 26.2 | 2739 | 9.2 | -0.9 |
| 10413-32.1 | 222 | 116 | 0.52 | 96 | 1.72E-5 | 4.46E-6 | 0.0003 | 0.1569 | 0.0032 | 12.632 | 0.142 | 0.5047 | 0.0053 | 0.9403 | 0.1815 | 0.0007 | 2634 | 22.8 | 2667 | 6.3 | 1.5 |
| 10413-35.1 | 360 | 160 | 0.44 | 166 | 2.02E-5 | 6.23E-6 | 0.0003 | 0.1318 | 0.0023 | 13.877 | 0.150 | 0.5365 | 0.0056 | 0.9607 | 0.1876 | 0.0006 | 2769 | 23.3 | 2721 | 4.9 | -2.2 |
| 10413-33.1 | 472 | 295 | 0.63 | 215 | --- | --- | 0.0000 | 0.1893 | 0.0037 | 13.509 | 0.192 | 0.5310 | 0.0073 | 0.9601 | 0.1845 | 0.0007 | 2746 | 30.6 | 2694 | 6.6 | -2.3 |
| 10413-34.1 | 551 | 87 | 0.16 | 169 | --- | --- | 0.0000 | 0.0475 | 0.0022 | 8.784 | 0.100 | 0.3573 | 0.0037 | 0.9130 | 0.1783 | 0.0008 | 1969 | 17.6 | 2637 | 7.7 | 29.3 |
| 10413-36.1 | 214 | 109 | 0.51 | 79 | 2.56E-5 | 3.51E-5 | 0.0004 | 0.1492 | 0.0037 | 10.064 | 0.131 | 0.4304 | 0.0051 | 0.9152 | 0.1696 | 0.0009 | 2308 | 23.1 | 2553 | 8.8 | 11.4 |

Notes (see Stern, 1997):

Spot name follows the convention x-y.z; where x = sample number, y = grain number and z = spot number. Multiple analyses in an individual spot are labelled as x-y.z.z

Uncertainties reported at 1sigma and are calculated by using SQUID 2.23.08.10.21, rev. 21 Oct 2008

f206$^{204}$ refers to mole percent of total 206Pb that is due to common Pb, calculated using the 204Pb-method; common Pb composition used is the surface blank (4/6: 0.05770; 7/6: 0.89500; 8/6: 2.13840)

* refers to radiogenic Pb (corrected for common Pb)

Discordance relative to origin = 100 * ((207/206 age -206/238 age)/(207Pb/206Pb age))

Calibration standard 6266; U = 910 ppm; Age = 559 Ma; 206Pb/238U = 0.09059

Error in $^{206}Pb/^{238}U$ calibration 1.0% (included) (GSC mount IP587)

Standard Error in Standard calibration was 0.34% (not included in above errors but required when comparing data from different mounts).

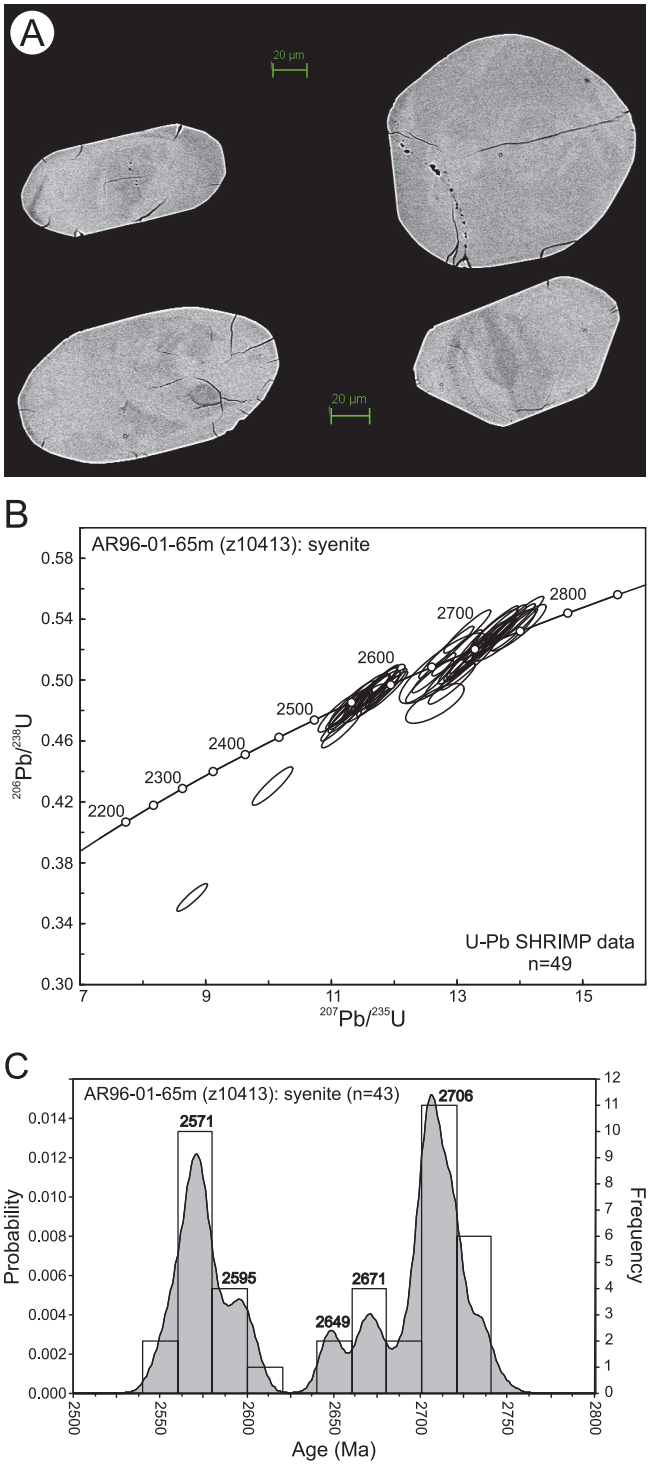


**Figure 3.** *A) BSE-SEM images of representative zircons from the Aucoin syenite (AR96-01-65 m: z10413), scale bars are 20 µm; B) U–Pb concordia diagram of zircon analyses from the syenite; and C) Cumulative probability plot of zircon ages from the syenite. Only analyses that are <5% discordant are included in this plot.*

inated by very-fine-grained, randomly oriented white mica (Figure 4A) that has been demonstrated using visible/infrared spectrometric analysis to be phengite (Sandeman and Rafuse, 2011). The phengite is typically ≤400 µm in long dimension, of suitable size to ensure a relatively pure mineral separate. The grain separate, therefore, represents a phengite concentrate and contains a small volume of other fine-grained mineral phases. These consist dominantly of albite and minor quartz and contain no appreciable $K_2O$ and will not contribute radiogenic $^{39}Ar$ to the step-heating age.

The criteria for a plateau were fully satisfied by the gas-release spectra for sample HS10-177B (Table 2; Figure 4). The phengite separate yielded a hump-shaped, somewhat irregular argon release spectrum (Figure 4B). The low apparent ages for the first three gas steps abruptly rise to a rough plateau for the remainder of the fractions. Each individual gas fraction is characterized by a relatively large error, thus the plateau age has a correspondingly large error. Gas release steps 4 through 21 yield a plateau age of 1873 ± 6 Ma, representing 86.9% of the $^{39}Ar$ released (MSWD = 0.85: POF = 0.63), overlapping, within error, the total gas integrated age of 1862 ± 12 Ma. This is interpreted as the time at which the phengite cooled through ~300°C (McDougall and Harrison, 1988; Reynolds, 1992) and hence the time of hydrothermal alteration of the syenite. The proximity of the sample of altered syenite to the Aucoin shear zone and its accompanying array of weakly sulphidic, auriferous quartz veins suggest that the alteration was synchronous with deposition of gold, silver and tellurium.

## PETROCHEMISTRY

### ANALYTICAL METHODS

Thirty seven lithogeochemical samples were obtained from rocks exposed at the Aucoin prospect. These include: eleven sulphide-poor and sulphide-bearing quartz veins; ten altered and fresh syenites; ten altered and fresh monzogabbros; one fine- to medium-grained monzodiorite that intrudes the syenite and; five northwest-trending diabase dykes. All specimens were submitted for determination of their major-, trace-, rare-earth element (REE) and gold pathfinder-element contents. Complete analytical methods are given in Sandeman (*in press*).

These data are supplemented by four relatively complete, lithogeochemical analyses published in mineral exploration assessment reports (Lehtinen and Weber, 1996; Hussey and Moore, 2005), as well as partial ICP-OES and Au fire assay results (Sandberg, 1995; Dyke and Hussey, 2003; Dyke, 2004; Hussey and Moore, 2006a, b). Samples of the diabase dykes are compared, where data is available,

**Table 2.** Aucoin argon data

| Sample | Mineral | | J | ± (1s) | % error | Lab # |
|---|---|---|---|---|---|---|
| HS10-177B | SER | | 0.005651 | 0.000022 | 0.389 | D-727r |
| Can/Pos | 222/40 | | | | | |

| | | Discrimination, extraction blank and decay corrected peak heights (mV) | | | | | | | | | | | Extraction blank peak heights (mV) | | | | | | |
|---|---|---|---|---|---|---|---|---|---|---|---|---|---|---|---|---|---|---|---|
| Step no | Power (%) | 40 | ± (1s) | 39 | ± (1s) | 38 | ± (1s) | 37 | ± (1s) | 36 | ± (1s) | Decay f37 | 40 | ± (1s) | 39 | ± (1s) | 38 | ± (1s) | 37 |
| 1 | 3.0 | 4972.920 | 4.521 | 18.252 | 0.274 | 1.156 | 0.145 | 1.482 | 0.491 | 0.995 | 0.087 | 4.16048 | 52.657 | 0.467 | 0.0243 | 0.0322 | 0.0229 | 0.0548 | 0.00532 |
| 2 | 4.0 | 31576.766 | 28.907 | 104.755 | 2.002 | 1.606 | 0.319 | 3.363 | 1.804 | 0.498 | 0.166 | 4.16165 | 52.172 | 0.463 | 0.0241 | 0.0319 | 0.0227 | 0.0543 | 0.00527 |
| 3 | 5.0 | 102721.067 | 66.225 | 325.000 | 4.001 | 4.009 | 0.821 | 3.249 | 4.919 | 0.774 | 0.347 | 4.16292 | 52.428 | 0.465 | 0.0242 | 0.0321 | 0.0228 | 0.0546 | 0.00530 |
| **4** | 6.0 | 52472.249 | 37.895 | 163.762 | 1.980 | 1.494 | 0.826 | 4.197 | 7.768 | 0.650 | 0.280 | 4.16768 | 52.428 | 0.465 | 0.0242 | 0.0321 | 0.0228 | 0.0546 | 0.00530 |
| **5** | 7.0 | 97933.884 | 70.629 | 309.751 | 4.070 | 3.232 | 0.845 | 2.142 | 3.837 | 0.493 | 0.467 | 4.16892 | 52.560 | 0.466 | 0.0242 | 0.0322 | 0.0228 | 0.0547 | 0.00531 |
| **6** | 7.9 | 88205.068 | 63.456 | 271.006 | 2.672 | 4.213 | 1.511 | 1.613 | 9.199 | 0.470 | 0.251 | 4.17034 | 52.428 | 0.465 | 0.0242 | 0.0321 | 0.0228 | 0.0546 | 0.00530 |
| **7** | 8.4 | 57099.114 | 47.966 | 179.603 | 2.250 | 2.584 | 0.551 | 1.052 | 3.185 | 0.043 | 0.246 | 4.17334 | 52.225 | 0.463 | 0.0241 | 0.0320 | 0.0227 | 0.0544 | 0.00528 |
| **8** | 8.9 | 49220.969 | 33.467 | 153.825 | 2.066 | 1.734 | 0.424 | 0.429 | 2.212 | 0.315 | 0.241 | 4.17497 | 51.730 | 0.459 | 0.0239 | 0.0317 | 0.0225 | 0.0538 | 0.00523 |
| **9** | 9.4 | 129774.666 | 93.400 | 400.222 | 3.959 | 4.415 | 1.605 | 11.288 | 17.093 | 0.204 | 0.158 | 4.17630 | 52.242 | 0.464 | 0.0241 | 0.0320 | 0.0227 | 0.0544 | 0.00528 |
| **10** | 9.9 | 69051.321 | 46.105 | 214.139 | 2.427 | 2.695 | 0.585 | 2.498 | 4.152 | 0.341 | 0.275 | 4.17769 | 52.242 | 0.464 | 0.0241 | 0.0320 | 0.0227 | 0.0544 | 0.00528 |
| **11** | 10.4 | 62967.285 | 43.840 | 193.946 | 2.152 | 2.778 | 0.516 | 0.177 | 2.628 | 0.026 | 0.203 | 4.17903 | 52.366 | 0.465 | 0.0242 | 0.0320 | 0.0228 | 0.0545 | 0.00529 |
| **12** | 10.9 | 101720.628 | 67.474 | 316.887 | 3.417 | 4.660 | 1.292 | 0.407 | 5.636 | 0.405 | 0.319 | 4.18034 | 52.887 | 0.469 | 0.0244 | 0.0324 | 0.0230 | 0.0550 | 0.00534 |
| **13** | 11.4 | 59596.133 | 50.109 | 186.973 | 2.525 | 2.329 | 0.481 | 0.227 | 2.918 | 0.304 | 0.190 | 4.18168 | 52.728 | 0.468 | 0.0243 | 0.0323 | 0.0229 | 0.0549 | 0.00533 |
| **14** | 12.0 | 29073.553 | 22.594 | 90.514 | 1.180 | 1.201 | 0.330 | 0.103 | 1.736 | 0.006 | 0.121 | 4.18302 | 52.021 | 0.462 | 0.0240 | 0.0318 | 0.0226 | 0.0541 | 0.00526 |
| **15** | 13.0 | 28144.915 | 40.489 | 85.958 | 0.540 | 1.482 | 0.727 | 0.001 | 0.985 | 0.019 | 0.088 | 6.31558 | 25.725 | 0.471 | 0.0394 | 0.0173 | 0.0267 | 0.0605 | 0.03017 |
| **16** | 13.6 | 29416.201 | 21.100 | 91.167 | 1.021 | 1.199 | 0.225 | 0.001 | 2.269 | 0.001 | 0.124 | 6.31754 | 25.725 | 0.471 | 0.0394 | 0.0173 | 0.0267 | 0.0605 | 0.03017 |
| **17** | 14.2 | 19643.472 | 17.231 | 60.331 | 0.881 | 0.774 | 0.194 | 0.938 | 1.393 | 0.096 | 0.098 | 6.31951 | 25.660 | 0.469 | 0.0393 | 0.0173 | 0.0266 | 0.0604 | 0.03010 |
| **18** | 14.9 | 26194.096 | 21.891 | 81.732 | 1.207 | 1.015 | 0.246 | 0.095 | 2.260 | 0.063 | 0.101 | 6.32323 | 25.565 | 0.468 | 0.0392 | 0.0172 | 0.0265 | 0.0602 | 0.02999 |
| **19** | 15.6 | 18780.906 | 16.770 | 57.807 | 0.692 | 0.651 | 0.148 | 0.001 | 1.876 | 0.085 | 0.097 | 6.32524 | 25.410 | 0.465 | 0.0389 | 0.0171 | 0.0263 | 0.0598 | 0.02980 |
| **20** | 16.6 | 19491.385 | 11.072 | 60.079 | 0.822 | 0.765 | 0.218 | 1.235 | 1.376 | 0.008 | 0.081 | 6.32726 | 25.695 | 0.470 | 0.0394 | 0.0173 | 0.0266 | 0.0605 | 0.03014 |
| **21** | 17.6 | 21459.813 | 14.515 | 65.775 | 0.837 | 0.955 | 0.205 | 0.363 | 1.418 | 0.001 | 0.097 | 6.32919 | 25.803 | 0.472 | 0.0395 | 0.0174 | 0.0267 | 0.0607 | 0.03026 |

**Footnotes:** **The following constants were used. All errors are 1-sigma**

All measurements were made using an MAP-216 mass spectrometer and the same electron multiplier maintained at a gain of 100 over the Faraday.
The same mass spectrometer operating conditions were used for all measurements. 1 mV ~ 4x10-13 cm3 (~1.9x10-17 moles).
Samples were irradiated at the McMaster reactor in position 8C without Cd shielding for 316 MWh. GA-1550 biotite and Hb3Gr hornblende (98.5 and 1074 Ma) were used as a flux monitors.
J values and errors for samples were determined by polynomial fit to replicate analyses of standards at measured positions along the length of the irradiation capsule.
Laser power is expressed as a % of maximum output power of a Merchantek MIR 10-30 CO2 laser (a facetted lens is used to diffuse the beam over 3 mm pits).

**Atmospheric Ar ratios:**

| | | ± (1s) | |
|---|---|---|---|
| 38/36Atms = | 0.1879 | 0.0003 | |
| 40/36Atms = | 295.5 | 0.031 | |
| Measured Atm | 283.18 | 1.20 | used for a linear discrimination correction. |

**Ratios used to correct for interfering isotopes:**

| | | ± (1s) | | | ± (1s) | | | ± (1s) | |
|---|---|---|---|---|---|---|---|---|---|
| 40/39K= | 0.03020 | 0.00091 | 39/37Ca= | 0.00070600 | 0.000028 | 36/37Ca= | 0.00027900 | 0.00001 | |
| 38/39K= | 0.01400 | 0.00000 | 38/37Ca= | 0.00003170 | 0.000000 | 36/39Ca= | 0.39518 | 0.020 | 36/38Cl= 320 |

**Decay Constants Used:**

| | | | |
|---|---|---|---|
| Lambda 40K = | 5.543E-10 | Lambda 39Ar = | 2.58E-03 (1/a) |
| Lambda 37Ar = | 7.2088 | Lambda 36Cl = | 2.30E-06 (1/a) |
| Blank corrected 39Ar was decay corrected usir | | 1.00051 | |

Both 37Ar and 39Ar decay corrections include the time in the reactor.

**Conversion factors:**

| | | ± (1s) |
|---|---|---|
| ClK fact = | 0.23 | 0.02 |
| CaK fact = | 1.83 | 0.085 |

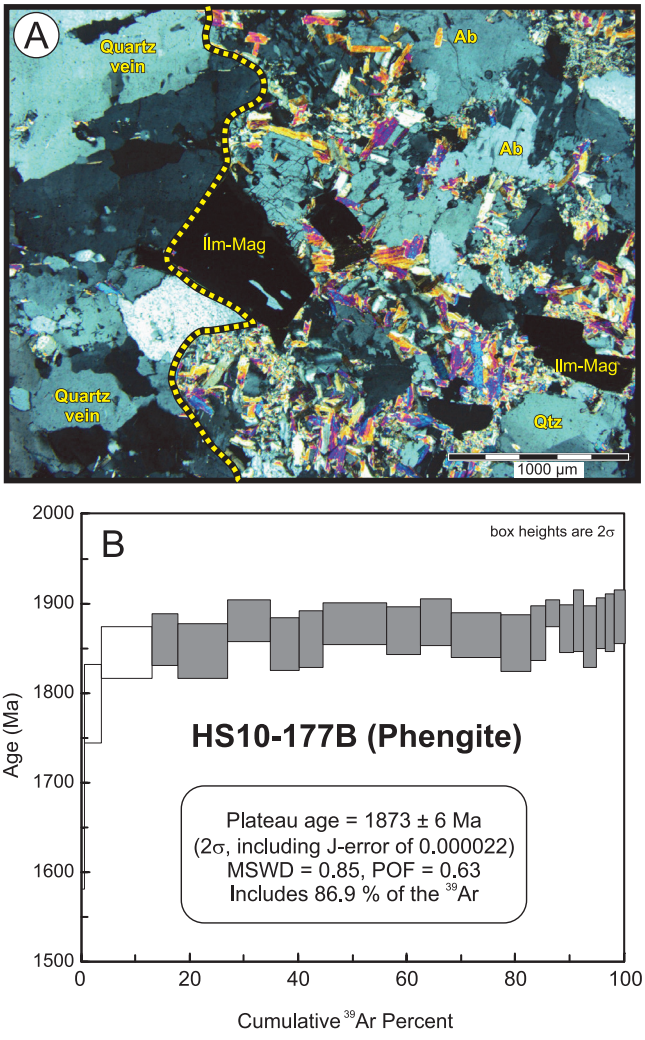


**Figure 4.** *A) Photomicrograph of syenite HS10-177B showing the extensive replacement of the matrix by intimately intergrown phengite (high birefringent laths), albite, quartz and magnetite-ilmenite. Note the quartz vein at left; and B) $^{40}Ar/^{39}Ar$ age spectrum for a phengite grain separate from syenite sample HS10-177B.*

to the KK subgroup of the Kikkertavak (dyke) swarm of Cadman *et al.* (1993). Dykes belonging to the CR subgroup of the Kikkertavak (dyke) swarm are lithogeochemically distinct from the diabase dykes in this investigation (Cadman *et al.*, *op. cit.*). The entire dataset is available in Sandeman (*in press*).

## COMMENTS ON ELEMENT MOBILITY AND ALTERATION

Alteration at the Aucoin prospect is typically restricted to rocks proximal to and structurally overlying the Aucoin shear zone. The shear zone and much of the structurally overlying syenite are typically characterized by abundant, northeast- and northwest-trending, locally sulphidic quartz veins and associated alteration (*e.g.*, Turpin showing and veins to southeast of Aucoin: Figure 2). Strong, chlorite–ankerite–epidote–talc±phengite alteration of the upper portions of the monzogabbro sill, and extensive phengite–carbonate alteration of the overlying syenite indicate that caution must be employed in the interpretation of the petrochemistry of these rocks. Altered examples show more variability in their $SiO_2$, $Al_2O_3$, CaO, $K_2O$, $Na_2O$ and large ion lithophile element (LILE: Rb, Sr, Ba, Cs) abundances than fresh rocks (Sandeman, *in press*). Fresh samples preserve less variable abundances of the major elements and LILE and appear to represent primary magmatic compositions. The immobile major and trace elements, along with the high-field strength (HFSE) and rare-earth elements (REE), show more systematic behaviour for all samples and these provide the firmest basis for petrogenetic interpretation of the rocks.

## COMMENTS ON ELEMENT ASSOCIATIONS IN MINERALIZATION

Whole-rock lithogeochemical sulphide-rich and sulphide-poor quartz vein samples, along with industry ICP and fire assay rock data from the Aucoin prospect and the affiliated Turpin showing are plotted in log-log plots (Figure 5). The data indicate that only the elements silver (Ag) and less so tellurium (Te) are correlated with gold (Au) at Aucoin (Figure 5). The extensive replacement of the ferromagnesian silicates as well as feldspars in the altered rocks by hydrous phases such as phengite, chlorite and talc, the elevated LOI (loss-on-ignition) contents of these rocks and relatively abundant secondary calcite indicate that an increase in volatile constituents is also a characteristic feature of the Aucoin alteration.

## ROCK CLASSIFICATION AND MAJOR- AND TRACE-ELEMENT VARIATIONS

Most of the fresh rocks, with the exception of the diabase dykes, are alkaline, quartz-poor to absent syenite, monzonite, monzodiorite/gabbro and feldspathoid-bearing monzodiorite/gabbro (ijolite or essexite: Figure 6A). Two samples of felsic rocks analyzed by Ascot Resources (Lehtinen and Weber, 1996) and Cornerstone Resources (Hussey and Moore, 2005) are alkali-feldspar granite and alkali-feldspar granite pegmatite, respectively. The monzogabbro exhibit elevated Nb/Y characteristic of alkali basalt, whereas the monzodiorite has lower Nb/Y. The syenite samples also have low Nb/Y but exhibit elevated $Zr/TiO_2$ typical of andesite and dacite (Figure 6B: Pearce, 1996). The five diabase dykes are basalts or gabbro (Figure 6A, B) and exhibit strong $FeO^T$ and $TiO_2$ enrichment with low Nb/Y ratios indicating that they are subalkaline, tholeiitic basalts (Pearce, 1996).

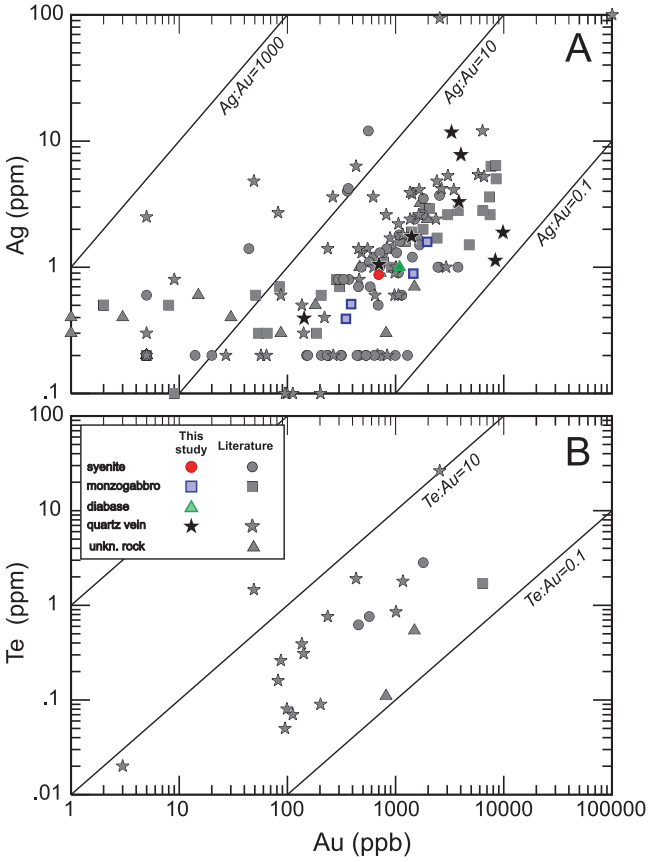


**Figure 5.** *Log-log plots for samples collected during this investigation compared to industry data. A) Ag* vs *Au; and B) Te* vs *Au.*

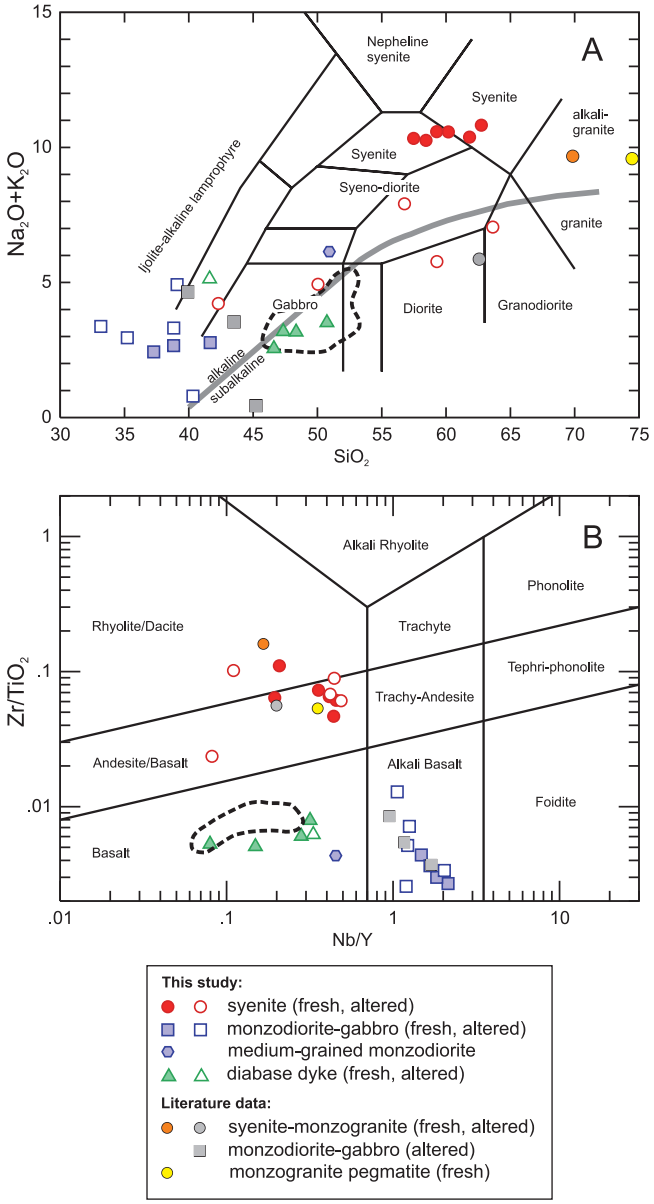


**Figure 6.** *Chemical classification of rocks hosting the Aucoin gold prospect. A) Total alkalies versus $SiO_2$ (wt. %) plutonic rock classification diagram (Wilson, 1989) and; B) $TiO_2/Zr$* vs *Nb/Y immobile element classification plot (Pearce, 1996). A field for, or alternatively where data is limited, individual samples of the KK dykes of Cadman* et al. *(1993) are shown for comparison.*

The paleotectonic setting of the rocks are tested using major- and trace-element discrimination diagrams. The monzogabbro, monzodiorite and syenite fall within the alkaline field in Figure 7A. The syenites plot in the calc-alkaline fields in Figure 7B and C, whereas the monzogabbros and monzodiorite are OIB to E-MORB in the Th–Zr–Nb diagram of Wood *et al.* (1979) and intercontinental rift to continental basalts in the La–Y–Nb diagram of Cabanis and Lecolle (1989). The diabase dykes fall within the MORB-continental tholeiite field in the V–Ti plot (Figure 7A: Shervais, 1982), are N-MORB–E-MORB varying to volcanic arc basalts in the Th–Zr–Nb diagram (Figure 7B: Wood *et al.*, 1979), whereas they are dominantly continental basalts ranging to volcanic arc basalts in the La–Y–Nb tectonic discrimination diagram (Figure 7C: Cabanis and Lecolle, 1989).

Selected major, compatible and incompatible trace elements for all Aucoin samples are plotted (Figure 8) against MgO wt.%. The fresh rocks define restricted clusters or arrays in major- and trace-element space. Fresh syenite has elevated $SiO_2$ (57.5-62.8 wt.%), $Al_2O_3$ (14.63-15.04 wt.%), $Na_2O$ (3.06-3.95 wt.%), $K_2O$ (6.43-7.56 wt.%) and $P_2O_5$ (0.48-1.10 wt.%) but lower concentrations of the other major elements relative to the monzodiorite/gabbro. Syenite exhibits linear negative correlation with MgO for most major and trace elements with the exception of $SiO_2$, $Na_2O$, $K_2O$, and Rb. Monzogabbro has low $SiO_2$ (33.2-41.8 wt.%) and $Al_2O_3$ (2.9-10.6 wt.%), variable MgO (5.2-19.7 wt.%), high $FeO^T$ (12.1-22.8 wt.%), strongly elevated $TiO_2$ (1.89-8.17 wt.%) and variable $Na_2O/K_2O$ (0.02-2.19) and LOI

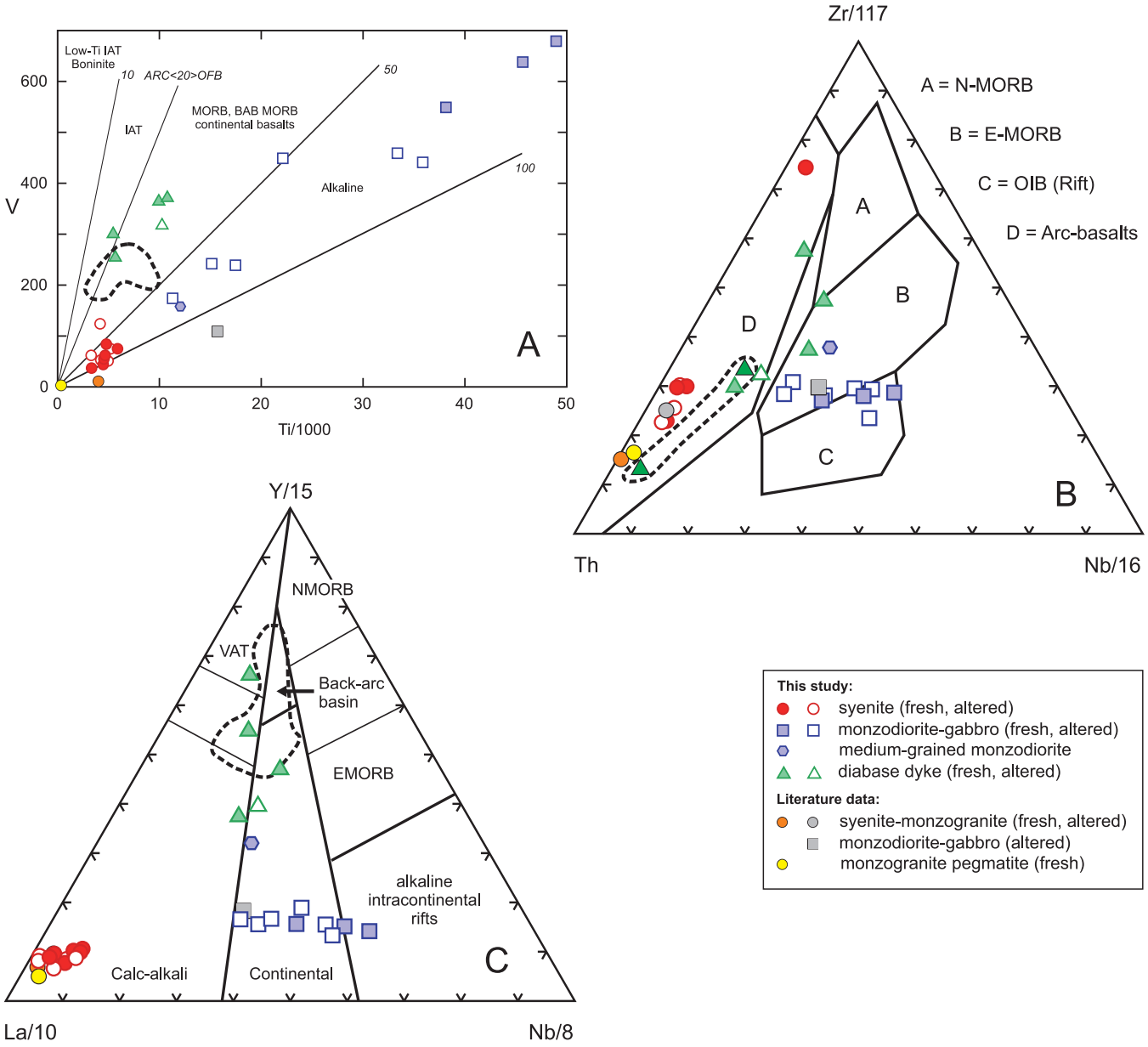


**Figure 7.** *Major- and trace-element, tectonic discrimination diagrams.* A) *V* vs *$TiO_2$/1000 diagram (Shervais, 1982);* B) *Th–Zr–Nb diagram (Wood* et al.*, 1979); and* C) *La–Y–Nb diagram (Cabanis and Lecolle, 1989). Dashed field is for the Kikkertavak dykes (Cadman,* et al., *1993).*

(0.39-12.5 wt.%). Altered monzogabbro is characterized by lower $TiO_2$ (1.38-5.98 wt.%: mean = 3.57 wt. %), $FeO^T$ (12.05-16.90 wt.%) and $Na_2O/K_2O$ (0.02-1.38: mean=0.84) but elevated volatiles (LOI = 1.41-12.5 wt.%: mean = 9.32 wt.%) whereas other major elements are at similar abundances to the fresh samples. The sample of medium-grained clinopyroxene–hornblende monzodiorite is distinct from monzogabbro in having higher $SiO_2$, $Al_2O_3$ and $Na_2O$, but lower MgO, CaO, $FeO^T$ and $TiO_2$.

The rare-earth element (REE) and incompatible trace-element abundances of the rocks are displayed as chondrite-normalized REE (Sun and McDonough, 1989: Figure 9A, C and E) and primitive mantle-normalized multi-element plots (Sun and McDonough, 1989: Figure 9B, D and F). All samples of each rock-type are mutually similar, defining closely grouped patterns (*see* Sandeman, *in press*; Figure 9). Altered specimens are, however, characterized by more variability in the large ion lithophile elements (LILE: Rb, Ba, Sr) as

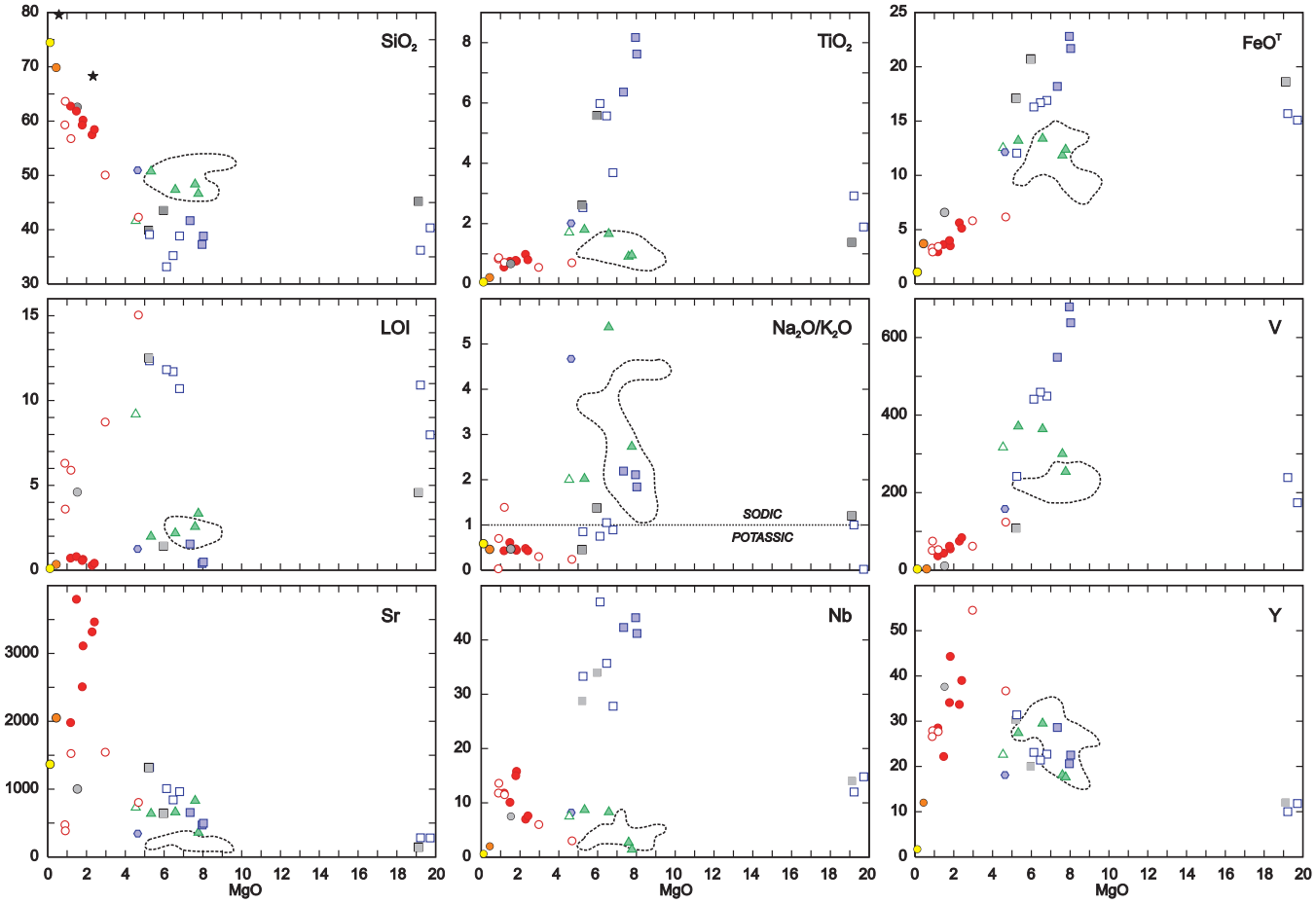


**Figure 8.** *Selected major and trace elements* versus *MgO wt. % for rocks of the Aucoin prospect. Symbols as in Figure 7.*

well as the high-field strength elements (HFSE) and, in particular, $TiO_2$.

The REE and multi-element patterns of the syenites, including altered samples, are also generally subparallel and define a tight field (*see* Sandeman, *in press*; Figure 9A, B). They have multi-element profiles that peak at La, and have very prominent Nb, P, Zr-Hf and Ti troughs. The rocks are strongly light-REE enriched ($[La/Yb]_{CN}$ = 63.50-108.83 $_{CN}$ denotes chondrite normalized after Sun and McDonough, 1989) and have a steep negative slope from the middle- to the heavy-REE ($[Gd/Yb]_{CN}$ = 8.30-11.91). The syenite has negligible to very modest negative Eu anomalies (Eu/Eu* = 0.88-1.00, mean = 0.92 :$Eu/Eu^* = Eu_{CN}/\sqrt{Sm_{CN} * Gd_{CN}}$). The monzogranite and monzogranite pegmatite have similar shaped REE and multi-element patterns, but have prominent positive Eu anomalies and also have the lowest incompatible trace-element contents of all of the silicic rocks.

With the exception of Y and the HREE, monzogabbro has incompatible trace-element concentrations significantly higher than average, normal mid-ocean ridge basalt (N-MORB: Sun and McDonough, 1989). They have convex upward multi-element profiles with peaks at Nb, steep negative slopes from Nb–Lu, notable P and minor Zr–Hf troughs and typically, enrichment of Nb and the LREE relative to Th (Figure 9C, D). Fresh samples have variably developed Ti spikes whereas altered rocks have variably developed troughs. The rocks are light-REE enriched ($[La/Yb]_{CN}$ = 13.07 to 20.42) and have a steep, negative slope from the middle- to the heavy-REE ($[Gd/Yb]_{CN}$ = 3.60-4.04). They exhibit very modest, positive and negative Eu anomalies (Eu/Eu* = 0.88-1.09, mean = 0.96).

The lone specimen of monzodiorite (HS10-188B) has a multi-element pattern generally similar to the monzogabbro (Figure 9C, D), however, it shows less light-REE enrichment ($[La/Yb]_{CN}$ = 7.84) and exhibits a more modest negative slope from the middle- to the heavy-REE ($[Gd/Yb]_{CN}$ = 2.88). The monzodiorite has a very minor negative Eu anomaly (Eu/Eu* = 0.96).

The northwest-trending diabase dykes appear to constitute 2 distinct petrochemical varieties on the basis of their REE and multi-element patterns (Figure 9E, F). Three of the five samples have inclined, modestly light-REE enriched

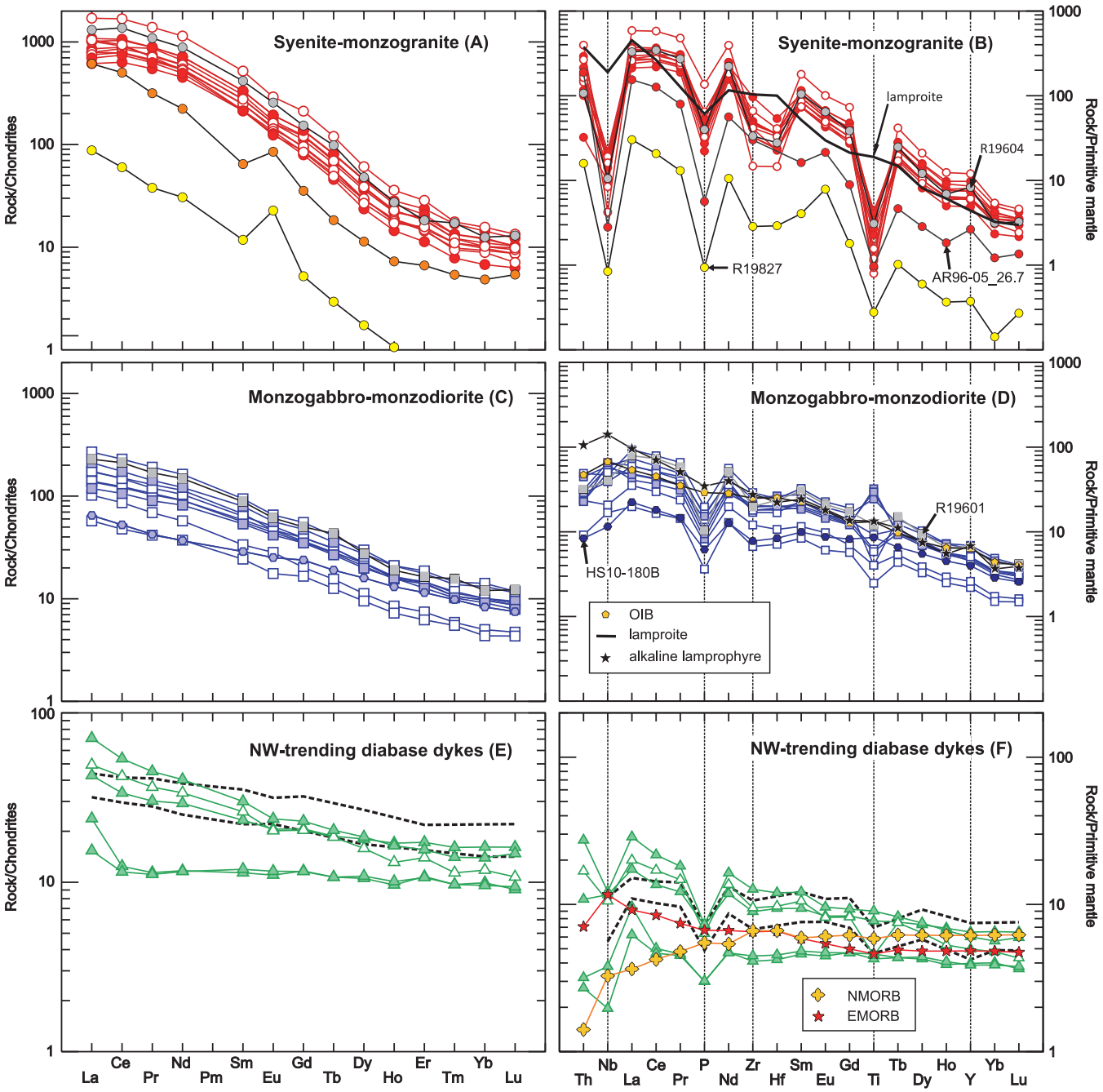


**Figure 9.** *Chondrite-normalized rare-earth element and primitive mantle-normalized multi-element plots (Sun and McDonough, 1989) for rocks of the Aucoin prospect. A, B) syenite and syenogranite; C, D) monzogabbro and monzodiorite, and; E,F) northwest-trending diabase dykes. Average, enriched mid-ocean ridge basalt (E-MORB), average normal mid-ocean ridge basalt (N-MORB) and oceanic island basalt (OIB: Sun and McDonough, 1989) as well as average alkaline lamprophyre and lamproite (Rock, 1991) are shown for comparison. Heavy dashed lines in E and F are 2 analyses of the KK dykes from Cadman* et al. *(1993). Symbols as in Figure 6.*

($[La/Yb]_{CN}$ = 2.64-5.09) profiles with variable negative Nb and P anomalies; one of these has a modest $TiO_2$ trough. The remaining two samples have generally flat multi-element profiles, with weak light-REE ($[La/Yb]_{CN}$ = 1.60-2.39) and middle- to heavy-REE ($[Gd/Yb]_{CN}$ = 1.18-1.21) enrichment, depletion in Th, Nb and P and very minor negative Eu anomalies (Eu/Eu* = 0.88-0.94, mean = 0.92).

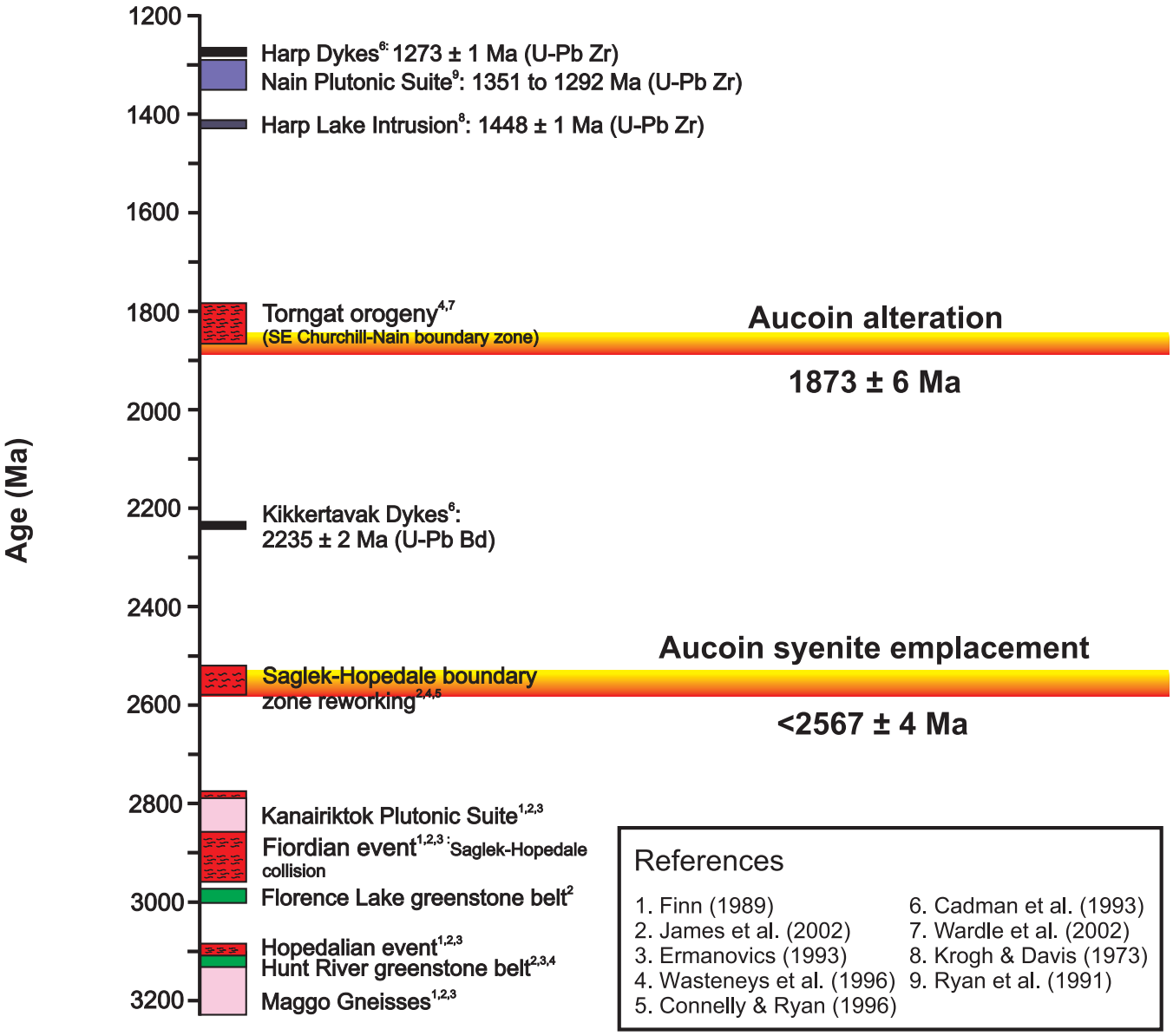


**Figure 10.** *Diagram summarizing geochronological constraints on the rocks at the Aucoin prospect as well as other salient constraints on the tectonic evolution of the Hopedale block of Labrador. The Archean events are largely based on James* et al. *(2002).*

## DISCUSSION

Field relationships at the Aucoin prospect indicate that the Au–Ag–Te mineralized quartz veins and associated alteration are hosted by four distinct rock types: *i.e.*, syenite–monzogranite, monzodiorite, monzogabbro and northwest–southeast-trending diabase dykes. All of these rocks have been altered and locally veined and mineralized. Variably altered syenite that co-hosts the Aucoin mineralization and alteration, cuts the Mesoarchean Maggo gneiss and yielded a maximum SHRIMP II U–Pb zircon age of 2567 ± 4 Ma. A specimen of phengite-altered syenite, obtained from the structural hanging wall of the prospect yielded a 14 step, $^{40}Ar/^{39}Ar$ step-heating plateau age of 1873 ± 6 Ma, overlapping, within error, with the total gas integrated age of 1862 ± 12 Ma. This is interpreted as the time at which the phengite cooled through ~300°C (McDougall and Harrison, 1988; Reynolds, 1992), and hence the time of hydrothermal alteration and deposition of precious-metal mineralization. Significantly, these new data indicate that the alkaline intrusive rocks exposed at the Aucoin prospect are not related to the mineralizing event as hypothesized by Hussey and Moore (2005) and Sandeman and Rafuse (2011). Instead, the precious-metal mineralization appears to represent a

structurally controlled, orogenic-type system of Paleoproterozoic age that is fortuitously hosted by these unusual, late Archean alkaline intrusive rocks. The Paleoproterozoic, in particular the interval from 1900–1750 Ma is well recognized as a period of major orogenic gold mineralization (Groves *et al.*, 2003). The Paleoproterozoic, *ca.* 1870 Ma age for Aucoin alteration and mineralization suggests the potential for the discovery of similar orogenic precious-metal systems along the western margin of the Nain craton, proximal to the Torngat orogenic front.

The Aucoin syenite is weakly silica-saturated, alkaline, strongly enriched in the highly incompatible and rare-earth elements and has prominent HFSE troughs. It is comparable to syenites generated in rift-related, intracontinental settings (*e.g.*, Riishuus *et al.*, 2005). Its mineralogy, LILE and LREE-enriched character and prominent HFSE troughs in multi-element plots indicate that the syenite is most similar to hydrous lamprophyric rocks such as lamproite and minette (Rock, 1991).

The monzodiorite dyke and monzogabbro sill at the Aucoin prospect are silica under saturated, alkalic, ocean-island-basalt-like, porphyritic mafic intrusive rocks that are slightly younger than the *ca.* 2567 Ma, cospatial syenite. Their hydrous modal mineralogy (abundant hornblende and less common biotite) indicates that they are not simple petrochemical equivalents of ocean island type basalt. Such hydrous-phase-rich, silica-poor mafic rocks are more typical of alkaline lamprophyres (Rock, 1991), rocks which are widely considered to be derived through low-degrees of partial melting of a volatile-rich ($CO_2$>$H_2O$), fertile, deep asthenospheric source. Less hydrous fertile mantle at similar depths, and slightly greater degrees of melting, will generate alkaline ocean island basalt in the Earth's ocean basins (Pearce, 2008; Presnall and Gudfinnsson, 2011). These points all suggest that at *ca.* 2570 Ma, a modestly hydrated, deep (≥90 km) mantle beneath the Hopedale block underwent partial melting to produce the primary magmas that ultimately yielded the Aucoin monzodiorite and monzogabbro. The syenite retains a distinct lithogeochemistry from the mafic alkaline rocks, and their full petrogenesis and relative association await further mineral, chemical and isotopic studies. Although not examined in detail, monzogranite and monzogranite pegmatite samples collected by industry appear to represent late-stage melts associated with the syenite and these have undergone feldspar accumulation.

Late Neoarchean ages are not common for rocks of the Nain Province. The few such determined ages (Schiotte *et al.*, 1992; Connelly and Ryan, 1996; Wasteneys *et al.*, 1996), ranging from 2578–2510 Ma are considered to record an interval of regional, granulite-facies-grade metamorphism and the coincident emplacement of small granitoid intrusions (Ermanovics and Ryan, 1990; Ermanovics, 1993; James *et al.*, 2002; Connelly and Ryan, 1996; Wasteneys *et al.*, 1996). This interval of metamorphism and plutonism was inferred to correspond to the time of late reworking of the Saglek–Hopedale boundary zone. If the Aucoin alkaline rocks were emplaced at *ca.* 2570 Ma, then this suggests that at that time, tectonic processes along the Saglek–Hopedale boundary zone may have involved transtension–transpression, enabling the local tapping of deep asthenospheric mantle below the western Hopedale block.

## ACKNOWLEDGMENTS

Andy Kerr is warmly thanked for his contribution of photographs and samples from the Aucoin prospect. Tim van Nostrand and his crew at Seal Lake kindly provided accommodation, food and companionship. Andrea MacFarlane and Jonathan Hull provided capable assistance in the field while Wayne Tuttle helped immensely with logistics and safety. The manuscript was improved by the helpful reviews of Andy Kerr and the staff of the Geoscience Publications and Information Section.

## REFERENCES

Black, L.P., Kamo, S.L., Allen, C.M., Davis, D.W., Aleinikoff, J.N., Valley, J.W., Mundil, R., Campbell, L.H., Korsch, R.J., Williams, L.S. and Foudoulis, C.

2005: Improved $^{206}Pb/^{238}U$ microprobe geochronology by the monitoring of a trace-element-related matrix effect; SHRIMP, ID-TIMS, ELA-ICP-MS and oxygen isotope documentation for a series of zircon standards. Chemical Geology, Volume 205, pages 115-140.

Brooks, C.

1982: Third report on the geochronology of Labrador pertaining to sub-project 109. Newfoundland Department of Mines and Energy, Open File Labrador 519.

1983: U-Pb geochronological ages. A report to Energy Mines and Resources concerning contract No. 1. EMP-MMD-82-0052 and amendment No. 1. Open File Labrador 519.

Cabanis, B. and Lecolle, M.

1989: Le diagramme La/10-Y/15-Nb/8: un outil pour la discrimination des series volcaniques et la mise en evidence des processus de melange et/ou de contamination crustale. Comptes Rendus de l'Acadamie des Sciences, Series II, Volume 309, pages 2023-2029.

Cadman, A.C., Heaman, L., Tarney, J., Wardle, R. and Krogh, T.E.

1993: U-Pb geochronology and geochemical variation within two Proterozoic mafic dyke swarms, Labrador.

Canadian Journal of Earth Sciences, Volume 30, pages 1490-1504.

Connelly, J. N., and Ryan, B.
1996: Late Archean evolution of the Nain Province, Nain, Labrador: imprint of a collision. Canadian Journal of Earth Sciences, Volume 33, pages 1325–1342.

Dalrymple, G.B., Alexander, Jr., E.C., Lanphere, M.A. and Kraker, G.P.
1981: Irradiation of samples for $^{40}Ar/^{39}Ar$ dating using the Geological Survey TRIGA Reactor. U.S. Geological Survey, Professional Paper 1176, 55 pages.

Dyke, B.
2004: Assessment report of lake sediment sampling, prospecting and rock sampling on Licences 8482M (2nd year), 9692M (1st year) and 9693M (1st year) Aucoin Property, NTS 13N/06, eastern Labrador, Newfoundland. NFLD 013N/06/0123.

Dyke, B. and Hussey, A.M.
2003: First year assessment report on compilation, prospecting and rock sampling on the Aucoin project Licence 8482M, NTS 13N/06, eastern Labrador, Newfoundland. NFLD 013N/06/0121.

Emslie, R.F.
1980: Geology and petrology of the Harp Lake Complex, central Labrador: an example of Elsonian magmatism. Geological Survey of Canada, Bulletin 293.

Ermanovics, I.
1993: Geology of Hopedale Block, southern Nain Province, and the adjacent Proterozoic terranes, Labrador, Newfoundland. Geological Survey of Canada, Memoir 431, 161 pages.

Ermanovics, I. and Ryan, B.
1990: Early Proterozoic orogenic activity adjacent to the Hopedale Block of southern Nain Province. Geoscience Canada, Volume 17, Number 4, pages 293-297.

Finn, G.C.
1989: Rb-Sr geochronology of the Archaean Maggo gneiss from the Hopedale block, Nain Province, Labrador. Canadian Journal of Earth Sciences, Volume 26, pages 2512-2522.

1991: Major-, trace-, and rare-earth-element geochemistry of the Archaean Maggo gneisses, southern Nain Province, Labrador. Canadian Journal of Earth Sciences, Volume 28, pages 44-57.

Friske, P.W.B., McCurdy, M.W., Gross, H., Day, S.J., Lynch, J.J. and Durham, C.C.
1993: Regional lake sediment and water geochemical reconnaissance data, eastern Labrador (NTS 13N). Geological Survey of Canada, Open File 2648.

Groves, D.I., Goldfarb, R.J., Robert, F. and Hart, C.J.R.
2003: Gold deposits in metamorphic belts: Overview of current understanding, outstanding problems, future research, and exploration significance. Economic Geology, Volume 98, pages 1-29.

Hill, J.D.
1982: Geology of the Flowers River – Natakwanon River area, Labrador. Mineral Development Division, Department of Mines and Energy, Government of Newfoundland and Labrador, Report 82-6, 140 pages.

Hornbrook, E.H.W. and Lund, N.G.
1978: Regional lake sediment and water geochemical reconnaissance data, Labrador. Geological Survey of Canada, Open File 558.

Hussey, A.M. and Moore, P.J.
2005: Assessment report of geology and lithogeochemistry on Licences 8482M (3rd yr.) and 9692M & 9693M (1st yr. supplementary), Aucoin Property, NTS 13N/06, Labrador. NFLD 013N/06/0129.

2006a: Fourth year assessment report of geology and geochemistry on mineral licence 8482M, Aucoin Property, NTS 13N/06, Labrador. NFLD 013N/06/0130.

2006b: Fifth year assessment report of geology and geochemistry on mineral licence 8482M, Aucoin Property, NTS 13N/06, Labrador. NFLD 013N/06/0131.

James, D.T., Kamo, S. and Krogh, T.
2002: Evolution of 3.1 and 3.0 Ga volcanic belts and a new thermotectonic model for the Hopedale Block, North Atlantic craton (Canada). Canadian Journal of Earth Sciences, Volume 39, pages 687-710.

Jourdan, F., Verati, C. and Féraud, G.
2006: Intercalibration of the Hb3gr $^{40}Ar/^{39}Ar$ dating standard. Chemical Geology, Volume 231, pages 77-189.

Kretz, R.
1983: Symbols for rock-forming minerals. American Mineralogist, Volume 68, pages 277-279.

Krogh, T.E.
1993: Report on Labrador geochronology, 1992-93. Newfoundland Department of Mines and Energy, Geological Survey Branch, Open File Labrador 997.

Krogh, T.E. and Davis, G.L.
1973: The significance of inherited zircons on the age and origin of igneous rocks – an investigation of the ages of the Labrador adamellites. Carnegie Institute of Washington Yearbook, Volume 72, pages 610-613.

Lehtinen, J.
1997: Geological, geophysical, geochemical and prospecting report on mineral licences 3895M and 5637M, Labrador (NTS 13N/5 and 13N/6). NFLD 013N/06/0079.

Lehtinen, J. and Weber, J.S.
1996: Geological, geophysical, geochemical and diamond drilling report on the Aucoin showing Ascot Property, Labrador (NTS 13N/05, 13N/06, mineral licence 3895M, 3896M & 4663M). NFLD 013N/06/0113.

Ludwig, K.R.
2003: User's manual for Isoplot/Ex rev. 3.00: a Geochronological Toolkit for Microsoft Excel. Special Publication, 4, Berkeley Geochronology Center, Berkeley, 70 pages.

2008: User's Manual for ISOPLOT 3.60 - A Geochronological Toolkit for Microsoft Excel. Berkeley Geochronological Centre Special Publication Number 4, 54 pages.

McDougall, I. and Harrison, T.M.
1988: Geochronology and thermochronology by the $^{40}$Ar-$^{39}$Ar method: Oxford Monographs on Geology and Geophysics #9, Oxford, United Kingdom, Oxford University Press, 212 pages.

Onstott, T.C., Phillips, D. and Pringle-Goodell, L.
1991: Laser microprobe measurement of chlorine and argon zonation in biotite. Chemical Geology, Volume 90, pages 145-168.

Pearce, J.A.
1996: A user's guide to basalt discrimination diagrams. *In* Trace Element Geochemistry of Volcanic Rocks; Applications for Massive Sulphide Exploration. Short Course Notes, Geological Association of Canada, Volume 12, pages 79-113.

2008: Geochemical fingerprinting of oceanic basalts with applications to ophiolite classification and the search for Archean oceanic crust. Lithos, volume 100, pages 14-48.

Presnall, D.C. and Gudfinnsson, G.H.
2011: Oceanic volcanism from the low-velocity zone without mantle plumes. Journal of Petrology, Volume 52, pages 1533-1546.

Reynolds, P.H.
1992: Low temperature thermochronology by the $^{40}$Ar-$^{39}$Ar method. *In* Low Temperature Thermochronology. *Edited by* M. Zentilli and P.H. Reynolds. Mineralogical Association of Canada, pages 3-19.

Riishuus, M. S., Peate, D.W., Tegner, C., Wilson, J.R., Brooks, C.K. and Waight, T.E.
2005: Petrogenesis of syenites at a rifted continental margin: origin, contamination and interaction of alkaline mafic and felsic magmas in the Astrophyllite Bay Complex, East Greenland. Contributions to Mineralogy and Petrology, Volume 149, pages 350-371.

Rock, N.M.S.
1991: Lamprophyres. Blackie and Son Ltd., Glasgow, 285 pages.

Roddick, J.C.
1983: High precision intercalibration of $^{40}$Ar/$^{39}$Ar standards. Geochimica et Cosmochimica Acta, Volume 47, pages 887-898.

Ryan, B.
1984: Regional geology of the central part of the Central Mineral Belt, Labrador. Mineral Development Division, Department of Mines and Energy, Government of Newfoundland and Labrador Memoir 3, 185 pages.

Ryan, B. (*Compiler*), Krogh, T.E., Heaman, L., Schärer, U., Philippe, S. and Oliver, G.
1991: On recent geochronological studies in the Nain Province and Nain Plutonic Suite, north-central Labrador. *In* Current Research. Newfoundland Department of Mines and Energy, Geological Survey Branch, Report 91-1, pages 257-261.

Sandberg, T.
1995: Report on prospecting program on map licences 3895M and 3896M, Labrador (NTS 13N/5 and 13N/6). NFLD LAB1147.

Sandeman, H.A.
*In press:* Lithogeochemical database for the Aucoin gold prospect, central Labrador (NTS map area 13N/6). Government of Newfoundland and Labrador, Department of Natural Resources, Geological Survey, Open File 013N/06/0143.

Sandeman, H.A. and Rafuse, H.
2011: The geological setting of Au-Ag-Te mineralization at the Aucoin prospect (NTS 13N/6) Hopedale Block, Labrador. *In* Current Research. Newfoundland Department of Mines and Energy, Geological Survey, Report 11-1, pages 167-183.

Schiotte, L., Nutman, A.P. and Bridgewater, D.
1992: U-Pb ages of single zircons within "Upernavik" metasedimentary rocks and regional implications for the tectonic evolution of the Archaean Nain Province, Labrador. Canadian Journal of Earth Sciences, Volume 29, pages 260-276.

Shervais, J.W.,
1982: Ti-V plots and the petrogenesis of modern and ophiolitic lavas, Earth and Planetary Science Letters, Volume 59 (1), pages 101-118.

Spell T.L. and McDougall, I.
2003: Characterization and calibration of $^{40}Ar/^{39}Ar$ dating standards. Chemical Geology, Volume 198, pages 189-211.

Steiger, R.H. and Jäger, E.
1977: Subcommission on geochronology: Convention on the use of decay constants in geo- and cosmochronology. Earth and Planetary Science Letters, Volume 36, pages 359-362.

Stern, R.A.
1997: The GSC Sensitive High Resolution Ion Microprobe (SHRIMP): analytical techniques of zircon U-Th-Pb age determinations and performance evaluation; in Radiogenic age and isotopic studies, Report 10. *In* Current Research, Part F. Geological Survey of Canada, Paper 97-1F, pages 1-31.

Stern, R.A. and Amelin, Y.
2003: Assessment of errors in SIMS zircon U-Pb geochronology using a natural zircon standard and NIST SRM 610 glass. Chemical Geology, Volume 197, pages 111-142.

Sun, S.S. and McDonough, W.F.
1989: Chemical and isotopic systematics of oceanic basalts: implications for mantle composition and processes. *In* Magmatism in the Ocean Basin. *Edited by* A.D. Saunders and M.J. Norry. Geological Society of London, Special Publication 42, pages 313-345.

Taylor, F.C. (compiler)
1977: Geology, Hopedale, Newfoundland. Map 1443A. Scale: 1:250 000. Geological Survey of Canada. Colour map. GS# 013N/0009.

Teskey, D.J., Dods, S.D. and Hood, P.J.
1982: Compilation techniques for the 1:1 million magnetic anomaly map series *In* Current Research, Part A. Geological Survey of Canada, Paper 82-1A, pages 351-358.

Thomas, A. and Morrison, R.S.
1991: Geological map of the central part of the Ugjoktok River (NTS 13N/5 and parts of 13M/8, and 13N/6), Labrador (with accompanying notes). Geological Survey Branch, Department of Mines and Energy, Government of Newfoundland and Labrador, Map 91-160.

Wardle, R. J., James, D. T., Scott, D. J., and Hall, J.
2002: The southeastern Churchill Province: synthesis of a Paleoproterozoic transpressional orogeny. Canadian Journal of Earth Sciences, Volume 39, pages 639-663. DOI: 10.1139/E02-004

Wasteneys, H., Wardle, R., Krogh, T. and Ermanovics, I.
1996: U-Pb geochronological constraints on the deposition of the Ingrid Group and implications for the Saglek-Hopedale and Nain craton – Torngat orogen boundaries. *In* Eastern Canadian Shield Onshore-Offshore Transect (ECSOOT). *Compiled by* R.J. Wardle and J. Hall. The University of British Columbia, Lithoprobe Secretariat, Report 57, pages 212-228.

Wilson, M.
1989. Igneous Petrogenesis. Unwin and Hyman, London, 466 pages.

Wood, D.A., Joron, J.L. and Treuil, M.
1979: A re-appraisal of the use of trace elements to classify and discriminate between magma series erupted in different tectonic settings. Earth and Planetary Science Letters, Volume 50, pages 326-336.